

On the Emergence of Weak-to-Strong Generalization: A Bias-Variance Perspective

Gengze Xu^{1*}, Wei Yao^{1*}, Ziqiao Wang^{2†}, Yong Liu^{1†}

¹Gaoling School of Artificial Intelligence, Renmin University of China,

²School of Computer Science and Technology, Tongji University,

{xugengze, wei.yao, liuyonggsai}@ruc.edu.cn ziqiaowang@tongji.edu.cn

Abstract

Weak-to-strong generalization (W2SG) refers to the phenomenon where a strong student model, trained on a dataset labeled by a weak teacher, ultimately outperforms the teacher on the target task. Recent studies attribute this performance gain to the prediction misfit between the student and teacher models. In this work, we theoretically investigate the emergence of W2SG through a generalized bias-variance decomposition of Bregman divergence. Specifically, we show that the expected population risk gap between the student and teacher is quantified by the expected misfit between the two models. While this aligns with previous results, our analysis removes several restrictive assumptions, most notably, the convexity of the student’s hypothesis class, required in earlier works. Moreover, we show that W2SG is more likely to emerge when the student model approximates its posterior mean teacher, rather than mimicking an individual teacher. Using a concrete example, we demonstrate that if the student model has significantly larger capacity than the teacher, it can indeed converge to this posterior mean. Our analysis also suggests that avoiding overfitting to the teacher’s supervision and reducing the entropy of student’s prediction further facilitate W2SG. In addition, we show that the reverse cross-entropy loss, unlike the standard forward cross-entropy, is less sensitive to the predictive uncertainty of the teacher. Finally, we empirically verify our theoretical insights and demonstrate that incorporating the reverse cross-entropy loss consistently improves student performance.

1 Introduction

Superalignment for large language models (LLMs) is emerging as a fundamental challenge in ensuring the long-term safety of modern natural language processing (NLP) systems [OpenAI, 2023]. A promising approach to addressing superalignment is weak-to-strong generalization (W2SG) [Burns et al., 2023], where a low-complexity weak teacher model generates pseudo-labels to supervise a high-complexity pre-trained strong student model, enabling the student to outperform the teacher on the target task. To theoretically understand the emergence of this phenomenon—why the student outperforms the teacher—recent advances in W2SG research propose several analytical frameworks [Ildiz et al., 2025; Wu and Sahai, 2025; Somerstep et al., 2025; Dong et al., 2025; Charikar et al., 2024; Mulgund and Pabbaraju, 2025; Yao et al., 2025b,a; Lang et al., 2024; Shin et al., 2025]. Among these, misfit-based analyses, initially introduced by Charikar et al. [2024], quantify the student’s performance gain in terms of the “misfit error” incurred when the student predicts labels produced by the teacher. While the original misfit analysis in Charikar et al. [2024] focuses on squared loss, Mulgund and Pabbaraju [2025] extends this analysis to a broader family of Bregman divergences via a generalized Pythagorean theorem.

However, previous misfit-based analyses have several limitations. Firstly, both Charikar et al. [2024] and Mulgund and Pabbaraju [2025] rely on a restrictive convexity assumption regarding the student’s function class, an assumption typically violated in practice, especially when all parameters of the student’s model are trainable. Although Mulgund and Pabbaraju [2025] partially relaxes this assumption by considering convex combinations within the student’s function class, it remains unclear whether one can entirely remove the convexity assumption from misfit-based W2SG inequalities. Secondly, while Mulgund and Pabbaraju [2025] suggests that reducing the misfit error facilitates W2SG, it does not clearly discuss the sense in which the student model should align with its teacher, nor does it explain why early stopping is important in practical W2S training. In addition, Charikar et al. [2024]; Mulgund and Pabbaraju [2025] often assume the ground-truth labeling function lies within the student’s hypothesis class, without explicitly analyzing why the student model typically needs to be larger than its teacher for W2SG to emerge. Finally, although reverse KL divergence appears as a misfit term in Mulgund

★ Equal contribution † Corresponding authors

and Pabbaraju [2025] and has been empirically studied in Yao et al. [2025a], a theoretical comparison between cross-entropy (CE) and reverse cross-entropy (RCE) within W2SG settings remains unexplored.

In this work, we present misfit-based W2SG inequalities by entirely removing the convexity assumption on the student’s hypothesis class. Specifically, our misfit-based analysis is conducted at the level of *expected population risk*, that is, the expected risk is evaluated over both data and model distributions, with loss functions based on Bregman divergences. This approach brings at least two benefits. First, it enables us to apply a generalized *bias-variance decomposition of Bregman divergences* recently developed by Pfau [2013]; Adlam et al. [2022], rather than relying on the generalized Pythagorean theorem, thereby avoiding the convexity assumption. In addition, explicitly analyzing expected population risk allows us to utilize the dependency between teacher and student models, an aspect overlooked in previous misfit analyses. As a result, our results suggest that an ideal scenario for W2SG occurs when the student’s predictions align with those of its “posterior mean” teacher, where the posterior is defined by conditioning the teacher’s distribution on the student model, and the mean may involve a dual expectation. From an algorithmic perspective, this insight encourages training student models using averaged labels from an ensemble of teachers. Furthermore, by specializing our results to squared loss and considering a ridge regression example, we show that reducing the expected misfit between teacher and student is sufficient for W2SG. Importantly, we find that this misfit term monotonically vanishes as the student’s model size increases. Intriguingly, we also demonstrate that overly minimizing this misfit (when its minimum value is zero), eliminates the performance gain, causing the student merely to replicate the teacher, which justifies the importance of regularization or early stopping in W2SG. Extending our analysis to the case where the Bregman divergence is the KL divergence (CE loss), we derive corresponding W2SG inequalities. We theoretically demonstrate that under CE or RCE loss, reducing the entropy of the student model’s predictions favors W2SG. Additionally, we provide a comparative theoretical analysis of CE and RCE in ideal scenarios, and we also show that RCE is significantly less sensitive to the teacher’s prediction confidence, an especially advantageous property when inputs are ambiguous for the teacher model.

After introducing the preliminaries, the remainder of the paper is organized as follows, along with a summary of our main contributions:

- In Section 3, we present our main theoretical result—the W2SG inequalities based on forward and reverse misfit errors (cf. Theorem 3.1) without the convexity assumption. We also highlight ideal scenarios where the performance gain depends solely on the misfit terms, demonstrating that aligning the student model with its posterior mean teacher ensures W2SG (cf. Corollary 3.1).
- In Section 4, focusing on squared loss and using a ridge regression example, we demonstrate that W2SG is more likely to emerge when the student has larger capacity (cf. Theorem 4.1).
- In Section 5, we provide W2SG inequalities for CE and RCE (cf. Corollary 5.1), suggesting that reducing the entropy (i.e., increasing confidence) of the student’s predictions facilitates W2SG. We also prove that using RCE as a misfit measure preserves the performance gains predicted by the reverse KL (cf. Proposition 1). As a by-product, we show that using RCE as the optimization objective mitigates issues associated with high uncertainty in the teacher’s predictions (cf. Proposition 2).
- In Section 6, we empirically estimate the bias and variance terms in W2SG to verify our theoretical insights. Specifically, we investigate how model size affects W2SG, and the effectiveness of supervising the student model with averaged predictions from multiple teachers. Additionally, by comparing CE and RCE under varying levels of teacher-label confidence, we discover an intriguing phenomenon: the performance of RCE remains robust even when the teacher’s labels are highly uncertain. Finally, we combining CE and RCE to further improve W2SG.

Other Related Literature To address the challenge of superalignment [OpenAI, 2023], a growing body of research has built upon the initial W2SG work by Burns et al. [2023], which empirically investigates the properties of W2SG [Shin et al., 2025; Yang et al., 2025; Goel et al., 2025; Yao et al., 2025b], and the potential of this paradigm on other tasks [Guo et al., 2024; Yang et al., 2024] or scenarios [Pawelczyk et al., 2024; Zhou et al., 2025]. Additionally, various techniques are also developed to enhance the strong model’s performance in W2SG, such as Lyu et al. [2025]; Ye et al. [2025]; Lang et al. [2025]; Agrawal et al. [2024]; Sang et al. [2024]; Liu and Alahi [2024]; Cui et al. [2025]. Although these methods show promising results, they often require additional weak models or involve complex computational procedures, leading to significant time and space overhead. In parallel, theoretical understanding of W2SG mainly focuses on whether it occurs, i.e., under what circumstances will the strong student outperform the weak teacher. From the perspective of a general definition of adversarial robustness, W2SG is proved to arise under appropriate data neighborhood conditions that enable weak supervision error correction [Lang et al., 2024] or sufficient overlap between easy and hard

patterns that allow weak supervision to guide the student in learning challenging features [Shin et al., 2025]. Under Gaussian data assumptions, the theoretical foundations of W2SG are rigorously characterized through several frameworks: model and distribution shift [Ildiz et al., 2025], benign overfitting [Wu and Sahai, 2025], transfer learning [Somerstep et al., 2025] and intrinsic dimension [Dong et al., 2025]. Further theoretical insights are established through representation analysis [Xue et al., 2025] and random feature model [Medvedev et al., 2025].

2 Preliminaries

Notations Throughout this paper, unless otherwise stated, capital letters (e.g., X) denote random variables, while the corresponding lowercase letters (e.g., x) denote their realizations. Let P_X be the distribution of X and $P_{X|Y}$ be the conditional distribution of X given Y . Conditioning on a specific realization is denoted by $P_{X|Y=y}$ or simply $P_{X|y}$. Expectations are expressed as $\mathbb{E}_X[\cdot]$. Similarly, $\mathbb{E}_{X|y}[\cdot]$ or $\mathbb{E}_X[\cdot | y]$ denotes expectation over $X \sim P_{X|Y=y}$.

Weak-to-Strong Generalization (W2SG) Setup Let \mathcal{X} and \mathcal{Y} denote the instance and label domains, respectively. In the weak-to-strong (W2S) setting, we consider two hypotheses classes $\mathcal{W} \subseteq \mathbb{R}^{d_w}$ and $\mathcal{W}' \subseteq \mathbb{R}^{d_s}$, with dimensions satisfying $d_s \geq d_w$. These hypothesis classes induce corresponding function classes: the weak model class $\mathcal{F} = \{f_w : \mathcal{X} \rightarrow \mathcal{Y} \mid w \in \mathcal{W}\}$, and the strong model class $\mathcal{F}' = \{f_{w'} : \mathcal{X} \rightarrow \mathcal{Y} \mid w' \in \mathcal{W}'\}$. We assume the existence of a ground-truth labeling function $g : \mathcal{X} \rightarrow \mathcal{Y}$. Suppose we have a pre-trained, high-capacity strong model $f_{w'_0} \in \mathcal{F}'$ and a weak model $f_w \in \mathcal{F}$, which may or may not be pre-trained. The weak model is trained on a dataset $S = \{(X_j, Y_j)\}_{j=1}^m$, drawn i.i.d. from an unknown distribution μ . To leverage the weak model’s supervision, we generate a pseudo-labeled dataset $S' = \{(X'_i, Y'_i)\}_{i=1}^n$, where $\{X'_i\}_{i=1}^n$ are drawn i.i.d. from $\mu_{\mathcal{X}}$ (which is the marginal distribution of X induced by μ) and each pseudo-label is obtained as $Y'_i = f_w(X'_i)$. Using this dataset, we fine-tune the pre-trained strong model $f_{w'_0}$ to obtain a final strong model $f_{w'}$. We say that weak-to-strong generalization (W2SG) occurs if this final strong model $f_{w'}$ estimates the ground-truth labeling function g better than its weak teacher f_w .

Remark 2.1 (Posterior Distribution of f_w). *The joint distribution of the teacher and student models, $P_{W, W'}$, is determined by: the marginal distribution of the teacher, P_W , which depends on the data distribution and other training randomness; and the conditional distribution $P_{W'|W}$, which captures the student’s training given the teacher, including the influence of S' and additional randomness such as pre-trained parameters W_0 . Consequently, the conditional distribution $P_{W|W'}$ is well-defined and referred to as the “posterior” distribution of the teacher.*

To formally quantify how well a model estimates the ground-truth labeling function, a suitable loss function is typically employed. We now introduce the Bregman divergence, a general class of divergences containing many popular loss functions.

Bregman Divergence Bregman divergences, an important class of divergences widely used in machine learning [Bregman, 1967; Banerjee et al., 2005], are defined as follows.

Definition 2.1 (Bregman [1967]). Let $\phi : \mathbb{R}^d \rightarrow \mathbb{R}$ be a differentiable, strictly convex function. The Bregman divergence generated by ϕ of $x, y \in \mathbb{R}^d$ is defined as $D_\phi(x, y) \triangleq \phi(x) - \phi(y) - \langle \nabla \phi(y), x - y \rangle$.

Common examples of Bregman divergences include the squared Mahalanobis distance, obtained by setting $\phi(x) = x^T M x$ for a positive semidefinite matrix $M \in \mathbb{R}^{d \times d}$ (which reduces to the squared loss or mean squared error if M is the identity matrix, i.e. $\phi(x) = \|x\|^2$) and the Kullback–Leibler (KL) divergence, obtained by setting $\phi(x) = \sum_i x_i \log x_i$.

Geometrically, the Bregman divergence measures the difference between the function ϕ and its supporting hyperplane at the point y . Although it generalizes the notion of a distance, sharing some metric-like properties such as non-negativity ($\forall x, y, D_\phi(x, y) \geq 0$) and the identity of indiscernibles ($\forall x, y, D_\phi(x, y) = 0$ if and only if $x = y$), it typically lacks symmetry and does not necessarily satisfy the triangle inequality. Instead, Bregman divergences obey a generalized law of cosines [Chen and Teboulle, 1993].

Let ϕ^* be the convex conjugate¹ of ϕ , and $x^* = \nabla \phi(x)$ be the dual representation of x under ϕ (we have $x = (x^*)^* = \nabla \phi^*(\nabla \phi(x))$ by properties of convex conjugation). Then, the generalized law of cosines for the Bregman divergence states that, for any $x, y, z \in \mathbb{R}^d$,

$$D_\phi(x, z) = D_\phi(x, y) + D_\phi(y, z) - \langle z^* - y^*, x - y \rangle. \quad (1)$$

Below are two important minimization properties of Bregman divergences derived from Eq. (1).

¹For a function $\phi : \mathcal{X} \rightarrow \mathbb{R} \cup \{-\infty, +\infty\}$, its convex conjugate is $\phi^*(y) \triangleq \sup_{x \in \text{dom}(\phi)} \langle x, y \rangle - \phi(x)$.

Lemma 2.1 (Banerjee et al. [2005]; Pfau [2013]). *Let X be a random variable over \mathbb{R}^d , and D_ϕ be any Bregman divergence over $\mathbb{R}^d \times \mathbb{R}^d$. The minimizers of the expected Bregman divergence from and to X satisfy the following equalities: (i) $\arg \min_{y \in \mathbb{R}^d} \mathbb{E} [D_\phi(X, y)] = \mathbb{E} [X]$. (ii) $\arg \min_{y \in \mathbb{R}^d} \mathbb{E} [D_\phi(y, X)] = \mathcal{E} [X]$, where $\mathcal{E} [X] \triangleq (\mathbb{E} [X^*])^*$ is the dual expectation as defined in Adlam et al. [2022] (i.e. $\nabla \phi(y) = \mathbb{E} [\nabla \phi(X)]$).*

Following Pfau [2013]; Adlam et al. [2022], Lemma 2.1 allows us to derive the following bias-variance decompositions for the Bregman divergence with respect to an arbitrary point y ,

$$\mathbb{E}_X [D_\phi(X, y)] = \mathbb{E}_X [D_\phi(X, \mathbb{E} [X])] + D_\phi(\mathbb{E} [X], y), \quad (2)$$

$$\mathbb{E}_X [D_\phi(y, X)] = D_\phi(y, \mathcal{E} [X]) + \mathbb{E}_X [D_\phi(\mathcal{E} [X], X)]. \quad (3)$$

In contrast to Mulgund and Pabbaraju [2025], our work relies on the decompositions in Eq. (2)–(3) rather than the generalized Pythagorean inequality, which marks a key methodological distinction.

Given a Bregman divergence as the loss function, we formally define the *expected population risk* of the teacher model f_W as $\mathbb{E}_{X,W} [D_\phi(g(X), f_W(X))]$, where X denotes an independent test sample. Since the Bregman divergence is generally asymmetric, we also define the corresponding *reverse population risk* as $\mathbb{E}_{X,W} [D_\phi(f_W(X), g(X))]$. The population risks for the student model are defined analogously. Both the population risk and reverse population risk serve as measures of how well a model approximates the ground-truth labeling function g .

3 W2SG through the Lens of Expected Misfit

We are now in a position to present our main results.

Theorem 3.1. *Under the teacher-student setting, the following inequalities hold,*

$$\mathbb{E} [D_\phi(g(X), f_{W'}(X))] \leq \mathbb{E} [D_\phi(g(X), f_W(X))] - \mathbb{E} [D_\phi(f_{W'}(X), f_W(X))] + \epsilon_1, \quad (4)$$

$$\mathbb{E} [D_\phi(f_{W'}(X), g(X))] \leq \mathbb{E} [D_\phi(f_W(X), g(X))] - \mathbb{E} [D_\phi(f_W(X), f_{W'}(X))] + \epsilon_2, \quad (5)$$

where

$$\begin{aligned} \epsilon_1 &= \sqrt{\mathbb{E} \|f_{W'}^*(X) - \mathbb{E} [f_W^*(X) | W', X]\|^2} \sqrt{\mathbb{E} \|g(X) - f_{W'}(X)\|^2}, \\ \epsilon_2 &= \sqrt{\mathbb{E} \|f_{W'}(X) - \mathbb{E} [f_W(X) | W', X]\|^2} \sqrt{\mathbb{E} \|g^*(X) - f_{W'}^*(X)\|^2}. \end{aligned}$$

Eq. (4) implies that the student can outperform the teacher—i.e., W2SG occurs—if ϵ_1 is sufficiently small. The potential performance gain is characterized by the *expected reverse misfit*, namely $\mathbb{E} [D_\phi(f_{W'}(X), f_W(X))]$, between the two models. Conceptually, the result in Eq. (4) aligns with the main result of Mulgund and Pabbaraju [2025] (cf. Theorem A.2 in Appendix). However, our analysis avoids many of their assumptions, including realizability, convexity, and sequential consistency, with the relaxation of the convexity condition being particularly notable. This is made possible by invoking the Bregman divergence decomposition in Eq. (3), rather than relying on the projection of the teacher model onto a convex hypothesis set of the student. In addition, Eq. (5) conveys an analogous message, but focuses on reverse population risks. Note that the *expected forward misfit*, namely $\mathbb{E} [D_\phi(f_W(X), f_{W'}(X))]$, in Eq. (5), when instantiated as cross-entropy (a surrogate for KL divergence), is the standard training loss used in practical W2SG setups. We will elaborate on this in Section 5.

Notably, Theorem 3.1 reveals a subtle trade-off in aligning the student model with the teacher. On one hand, since the student lacks access to the ground-truth labels, it must rely on the pseudo labels provided by the teacher. That is, minimizing the empirical risk with respect to the teacher’s outputs, e.g., $\frac{1}{n} \sum_{i=1}^n D_\phi(f_w(x_i), f_{w'}(x_i))$, becomes a necessary part of training. On the other hand, Eq. (4) and Eq. (5) suggest that the expected misfit between the teacher and the student models contributes directly to the performance improvement of the strong student over the weak teacher. In particular, greater misfit between the two models can indicate a larger performance gain achieved by the student, which also align with a recent argument given in Dong et al. [2025]. This suggests that a pointwise alignment of $f_{w'}$ with f_w may be undesirable. Consequently, incorporating regularization or applying early stopping to prevent $\frac{1}{n} \sum_{i=1}^n D_\phi(f_w(x_i), f_{w'}(x_i))$ from converging to zero is not only consistent with practical strategies adopted in Burns et al. [2023], but also theoretically justified.

Theorem 3.1 also hints conditions under which ϵ_1 and ϵ_2 vanish, leading to the following results.

Corollary 3.1. *Under the teacher-student setting, if $f_{W'}(x) = \mathcal{E} [f_W(x) | W']$ for $\forall x \in \mathcal{X}$, then*

$$\mathbb{E} [D_\phi(g(X), f_{W'}(X))] = \mathbb{E} [D_\phi(g(X), f_W(X))] - \mathbb{E} [D_\phi(\mathcal{E} [f_W(X) | W', X], f_W(X))]. \quad (6)$$

Furthermore, if $f_{W'}(x) = \mathbb{E}[f_W(x)|W']$ for $\forall x \in \mathcal{X}$, then

$$\mathbb{E}[D_\phi(f_{W'}(X), g(X))] = \mathbb{E}[D_\phi(f_W(X), g(X))] - \mathbb{E}[D_\phi(f_W(X), \mathbb{E}[f_W(X)|W', X])]. \quad (7)$$

Corollary 3.1 presents situations where W2SG is guaranteed to emerge: specifically, when the student’s prediction matches that of its (dual) “posterior” mean teacher, where the (dual) expectation is taken with respect to $P_{W|W'}$ (i.e. the posterior distribution of teacher model, as discussed in Remark 2.1). Moreover, it is worth noting that both the forward and reverse misfit terms attain their minimum values in Eq. (6) and Eq. (7). These terms become zero when there is a single fixed teacher model (i.e., $|W| = 1$), or more generally, when $P_{W|w'}$ is a Dirac distribution, indicating a unique possible teacher model for each given student. In such cases, the performance gain vanishes, and aligning the student model perfectly with its posterior mean teacher—equivalent to pointwise fitting here—may become undesirable for W2SG to emerge.

Corollary 3.1 indicates that as the student model approaches its posterior mean teacher, both the residual terms (e.g., ϵ_2) and the expected misfit terms decrease. In the next section, we will demonstrate that reducing the expected misfit can serve as a sufficient condition for driving ϵ_1 and ϵ_2 to zero.

4 Symmetric Bregman Divergence: Squared Loss

Theorem 3.1 suggests that W2SG arises when the student model approximates the posterior mean teacher, either in the dual space, as indicated by Eq. (4), or in the primal space, as in Eq. (5). We now investigate the conditions under which the student model becomes close to its posterior mean teacher, thereby driving ϵ_1 and ϵ_2 to zero.

Specifically, in this section, we consider $\phi(x) = \|x\|^2$, i.e., squared loss, in which case $\epsilon_1 = \epsilon_2$. The following result is a special case of Theorem 3.1.

Corollary 4.1. *Let $\phi(x) = \|x\|^2$, then the following inequality holds,*

$$\mathbb{E}\|g(X) - f_{W'}(X)\|^2 \leq \mathbb{E}\|g(X) - f_W(X)\|^2 - \mathbb{E}\|f_{W'}(X) - f_W(X)\|^2 + \epsilon_2,$$

$$\text{where } \epsilon_2 = 2\sqrt{\mathbb{E}\|f_{W'}(X) - \mathbb{E}[f_W(X) | W', X]\|^2} \sqrt{\mathbb{E}\|g(X) - f_{W'}(X)\|^2}.$$

To analyze when ϵ_2 becomes small, we focus on the quantity $\mathbb{E}\|f_{W'}(X) - \mathbb{E}[f_W(X) | W', X]\|^2$, rather than directly analyzing the expected distance between the student model and ground truth labeling function, i.e. $\mathbb{E}\|g(X) - f_{W'}(X)\|^2$, which is also a component of ϵ_2 . For any input $x \in \mathcal{X}$,

$$\mathbb{E}\|f_{W'}(x) - \mathbb{E}[f_W(x) | W']\|^2 = \underbrace{\mathbb{E}\|f_{W'}(x) - f_W(x)\|^2}_{\text{Expected Misfit}} - \underbrace{\mathbb{E}\|f_W(x) - \mathbb{E}[f_W(x) | W']\|^2}_{\text{Conditional Variance of } f_W}. \quad (8)$$

Remark 4.1. *The expected misfit term here corresponds to the standard population risk on the data distribution induced by μ_X and the “ground-truth” labeling function f_W . In this view, the total variance $\mathbb{E}\|f_W(x) - \mathbb{E}[f_W(x)]\|^2$ can be interpreted as the “Bayes error”, while the conditional variance term in Eq. (8) underestimates it [Adlam et al., 2022, Proposition 4.1].*

Notably, due to the presence of the conditional variance, we can see that ϵ_2 vanishes before the expected misfit does, in other words, the vanishing of the expected misfit term is a sufficient condition for ϵ_2 to vanish. Furthermore, recent studies on the “double descent” phenomenon show that this expected misfit, when regarded as the population risk, can indeed decrease as the capacity of the student model increases [Belkin et al., 2019; Hastie et al., 2022; Mei and Montanari, 2022; Yang et al., 2020; Ba et al., 2020]. We now formalize this through the following example.

Example 1 (Ridge Regression). Assume $X \sim \mathcal{N}(0, \mathbf{I}_{d_w}/d_w)$, and let the teacher model be $f_w(x) = x^T w$ for $w \in \mathbb{R}^{d_w}$ and the student model be $f_{w'}(x) = (w'_1 x)^T w'_2$, where² $w'_1 \in \mathbb{R}^{d_s \times d_w}$ and $w'_2 \in \mathbb{R}^{d_s}$. The weights W'_1 are initialized with entries drawn i.i.d. from $\mathcal{N}(0, 1/d_w)$ and remain fixed during training. The student is trained via ridge regression: $\min_{w'_2} \|(w'_1 \mathbf{x}')^T w'_2 - \mathbf{y}'\| + \eta \|w'_2\|^2$ where $\mathbf{x}' = [x'_1, \dots, x'_n] \in \mathbb{R}^{d_w \times n}$ and $\mathbf{y}' = [y'_1, \dots, y'_n] \in \mathbb{R}^n$.

Building on the random matrix theory-based analysis of double descent [Hastie et al., 2022; Mei and Montanari, 2022; Ba et al., 2020], and in particular the randomized-design setting in Yang et al. [2020], we derive the following asymptotic result.

²Here d_s refers to the number of hidden units rather than the total number of parameters.

Theorem 4.1. Assume $\mathbb{E}\|W\|^2 \leq B$ for some constant $B \in (0, \infty)$, and there exists $\gamma \in (1, \infty)$ s.t. $\frac{d_s}{d_w} \rightarrow \gamma$ as $d_s, d_w \rightarrow \infty$, and $\frac{n}{d_w} \rightarrow \infty$ as $n, d_w \rightarrow \infty$. Let $\eta = \frac{n}{d_w}\eta_0$ for some fixed $\eta_0 > 0$. Then, as $n, d_s, d_w \rightarrow \infty$, the following bound holds a.s.,

$$\mathbb{E}\|f_{W'}(X) - f_W(X)\|^2 \leq Bh(\eta_0, \gamma),$$

where $h(\eta_0, \gamma) = \frac{\eta_0(\gamma+1)+(\gamma-1)^2}{2\sqrt{\gamma^2-2(1-\eta_0)\gamma+(\eta_0+1)^2}} - \frac{\gamma-1}{2}$.

Remark 4.2. Notably, as $\eta_0 \rightarrow 0$, we have $h(\eta_0, \gamma) \rightarrow 0$ and consequently $\epsilon_2 \rightarrow 0$. However, as discussed in Section 3, allowing the student to interpolate the teacher-labeled data is undesirable in practice, as it eliminates the potential performance gain and prevents W2SG from emerging. From this perspective, maintaining $\eta_0 \neq 0$ is essential. In fact, for any fixed $\eta_0 > 0$, the function $h(\eta_0, \gamma)$ decreases monotonically with γ . Hence, W2SG emerges when γ becomes sufficiently large (i.e. the student model becomes large enough) so that $h(\eta_0, \gamma)$ equals to the conditional variance of f_W , in which case $\epsilon_2 \rightarrow 0$ while $\mathbb{E}\|f_{W'}(X) - f_W(X)\|^2 \neq 0$.

Example 1 and Theorem 4.1 can be extended to more complex architectures, such as nonlinear neural networks, by utilizing the analysis in Ba et al. [2020]. To summarize, W2SG is more likely to emerge under the following conditions: 1) The student model size should be sufficiently large (i.e., large γ), though the performance gain eventually saturates; 2) The student should not interpolate the teacher’s labels (i.e., zero training loss is undesirable), requiring regularization or early stopping during W2S training (i.e., $\eta_0 \neq 0$). These insights have not been explicitly highlighted in previous misfit-based analyses Charikar et al. [2024]; Mulgund and Pabbaraju [2025], which typically assume that the ground-truth labeling function lies within the student’s hypothesis class (i.e., $g \in \mathcal{F}'$) without discussing why a larger student model is necessary.

While we have shown that increasing the student model size drives ϵ_2 and ϵ_1 towards zero—i.e., the student converges to its posterior mean teacher—thus enabling W2SG to emerge under a symmetric Bregman divergence loss (specifically, squared loss), we conjecture that a similar result holds for asymmetric Bregman divergences as well. However, providing a theoretical justification for this is challenging. One potential obstacle is the lack of formal theoretical analyses characterizing double descent behavior under cross-entropy loss, despite its well-documented empirical evidence Nakkiran et al. [2020].

5 Asymmetric Bregman Divergence: From (reverse) KL to (reverse) CE

In this section, we focus on a K -class classification task, where $\mathcal{Y} \subset \mathbb{R}^K$ and $\|y\|_1 = 1$ for all $y \in \mathcal{Y}$. In practical training, a commonly used loss function is the (forward) CE loss [Burns et al., 2023], defined as $\text{CE}(y, \hat{y}) \triangleq -\sum_{i=1}^K y_i \log \hat{y}_i$ for any $y, \hat{y} \in \mathcal{Y}$. Since $\text{CE}(y, \hat{y}) = \text{D}_{\text{KL}}(y||\hat{y}) + H(y)$, where $\text{D}_{\text{KL}}(y||\hat{y}) \triangleq \sum_{i=1}^K y_i \log \frac{y_i}{\hat{y}_i}$ is the KL divergence and $H(y) = -\sum_{i=1}^K y_i \log y_i$ is the Shannon entropy, and given that KL divergence is a special case of Bregman divergence, we have:

Corollary 5.1. Let $\phi(x) = \sum x_i \log x_i$ and define the reverse cross-entropy (RCE) as $\text{RCE}(y, \hat{y}) \triangleq -\sum_{i=1}^K \hat{y}_i \log y_i$ for any $y, \hat{y} \in \mathcal{Y}$, the following inequalities hold,

$$\begin{aligned} \mathbb{E}[\text{CE}(g(X), f_{W'}(X))] &\leq \mathbb{E}[\text{CE}(g(X), f_W(X))] - \mathbb{E}[\text{RCE}(f_W(X), f_{W'}(X))] + \mathbb{E}[H(f_{W'}(X))] + \epsilon_1, \\ \mathbb{E}[\text{RCE}(g(X), f_{W'}(X))] &\leq \mathbb{E}[\text{RCE}(g(X), f_W(X))] - \mathbb{E}[\text{CE}(f_W(X), f_{W'}(X))] + \mathbb{E}[H(f_{W'}(X))] + \epsilon_2, \end{aligned}$$

where ϵ_1, ϵ_2 are defined as in Theorem 3.1.

Notably, both inequalities in Corollary 5.1 involve the entropy of the student’s prediction, $H(f_{W'}(X))$. This implies that, when CE (either forward one or reverse one) is used to measure population risk, reducing the entropy of the student’s output distribution favors the emergence of W2SG. In other words, high-confidence predictions by the student (i.e., low predictive uncertainty) are beneficial for outperforming the teacher. In fact, the original W2SG paper [Burns et al., 2023] adopts a regularized loss of the form

$$\mathcal{L}_{\text{AUX}} = \beta \text{CE}(f_w(x), f_{w'}(x)) + (1 - \beta) \text{CE}(f_{w'}(x), \hat{f}_{w'}(x)), \quad (9)$$

where $\hat{f}_{w'}(x)$ is the hardened prediction of the student³ so $\hat{f}_{w'}(x)$ is a one-hot vector. This regularization explicitly encourages entropy minimization, consistent with the implications of Corollary 5.1.

³Note that a confidence threshold is applied in [Burns et al., 2023, Eq. (1)] to decide whether to harden the prediction.

Furthermore, evaluating the quality of a trained model using the forward CE is the de facto standard in practice, then according to Corollary 5.1, minimizing RCE between the teacher and student appears more natural. As conjectured at the end of Section 4, this may help reduce ϵ_1 and thereby facilitate W2SG. Empirical studies by Yao et al. [2025a] have also advocated reverse KL for its mode-seeking property, which benefits strong model performance. We now proceed to elaborate on the comparison between CE and RCE as objective functions in W2S training.

In the idealized setting where both ϵ_1 and ϵ_2 vanish, we obtain the following result:

Proposition 1. *Under the ideal conditions of Corollary 3.1 where ϵ_1 and ϵ_2 vanish, the performance gain in the first inequality of Corollary 5.1 coincides with Eq. (6), while the gain in the second inequality is strictly smaller than Eq. (7).*

This suggests that evaluating the population risk using forward CE, while aligning the student to the teacher via RCE, preserves the performance gains predicted by Corollary 3.1. Moreover, RCE provides additional notable advantages when the teacher’s predictions exhibit low confidence (i.e., high uncertainty), as illustrated below.

Proposition 2. *Given a data distribution $\mu = \mu_X \mu_{Y|X}$ and any $\alpha \in [0, 1]$, we define a label-shifted distribution $\hat{\mu} = \mu_X \mu_{\hat{Y}|X}$ by smoothing the labels as follows: for each $(X, Y) \sim \mu$, the smoothed label is given by $\hat{Y}_j = \frac{1}{2} + \alpha(Y_j - \frac{1}{2})$ for $\forall j \in [2]$. If RCE is used as the loss function in binary classification, then the population risk minimizer on $\hat{\mu}$ also minimizes the population risk on μ .*

Note that decreasing α increases the uncertainty of the smoothed label \hat{Y} but does not affect its hard (argmax) label. If \hat{Y} represents the label provided by the teacher model, Proposition 2 shows that the RCE loss is less sensitive to the teacher’s confidence levels. This property is especially desirable when the input x is ambiguous for the teacher. Furthermore, in Appendix D.4, we demonstrate that uncertain weak supervision can lead to vanishing gradients under standard CE, whereas RCE maintains gradient stability. Later on we will empirically demonstrate how to leverage the advantages of RCE in scenarios involving low-confidence predictions.

6 Experiments

In this section, we present empirical studies on W2SG. Specifically, we aim to verify the key insights from our theoretical analysis, visualize the bias and variance terms in W2SG, and compare the effects of using CE and RCE as training objectives. Additionally, we further propose a novel training objective to improve the performance of W2SG.

Datasets Our experiments employ diverse datasets covering both standard NLP tasks and LLM reward modeling tasks. For standard NLP tasks, we utilize the SciQ [Welbl et al., 2017], Amazon Polarity [McAuley and Leskovec, 2013] and Twitter Sentiment ⁴ datasets, following the experimental setup of Burns et al. [2023] to transform these datasets into binary classification tasks. For reward modeling tasks, we sample subsets from CAI-Harmless [Bai et al., 2022b] and HH-RLHF [Bai et al., 2022a], with experimental settings referencing Yang et al. [2025], to guide models toward achieving harmlessness or helpfulness objectives.

Models We conduct our experiments based on the GPT-2 series of models [Radford et al., 2019], including GPT2, GPT2-Medium, GPT2-Large, and GPT2-XL. We add a linear projection layer atop the pretrained model, followed by an activation function to obtain prediction probabilities. Notably, we adopt a full fine-tuning strategy during training without freezing any pretrained parameters.

Emergence of W2SG We empirically investigate several insights from our theoretical framework in the context of LLMs: 1) The conditions for W2SG to emerge, as outlined in Theorem 3.1 and Corollary 3.1; 2) How the strong model’s capacity influences W2SG, as discussed in Theorem 4.1 and Remark 4.2. To further deepen our understanding of these phenomena in these two scenarios, we also systematically investigate how bias and variance affect the strong model’s performance. For the first insight, we independently train multiple weak teachers and compute their average prediction to approximate the dual expectation term in Corollary 3.1. We employ Algorithm 1 [Yang et al., 2020] for bias and variance estimation. For the second one, we use a probability-based ensemble [Dietterich, 2000; Zhou, 2025] of independently trained GPT2 models as the weak teacher and progressively scale the strong model’s capacity (GPT2-Medium, GPT2-Large, and GPT2-XL). The results are shown in Figure 1.

⁴<https://www.kaggle.com/datasets/jp797498e/twitter-entity-sentiment-analysis>

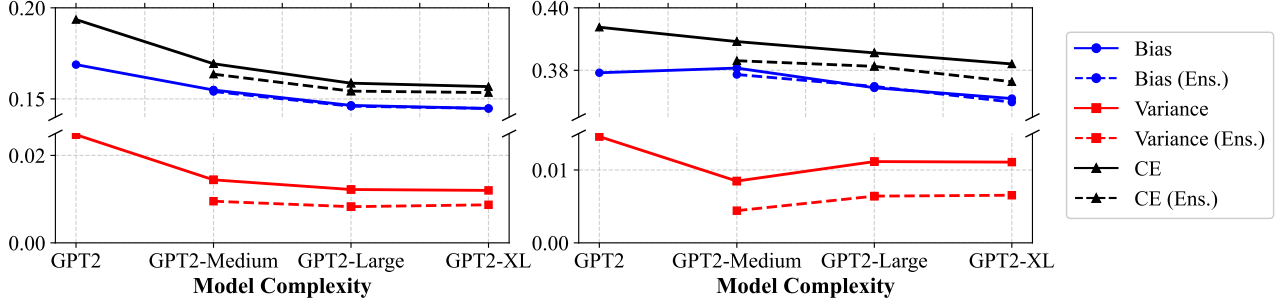


Figure 1: Bias and variance estimation on Amazon Polarity (left) and Twitter Sentiment (right). GPT-2 is trained as the teacher and used to supervise the three strong students’ model training. “CE” represents cross-entropy test loss. “Ens.” represents student performance supervised by expected teacher, approximated via weak teachers ensemble in dual space.

Conditional expectation estimation makes W2SG emerge. As expected, when using model ensembles to approximate the (dual) expected teacher in Corollary 3.1, we observe a consistent reduction in the test loss of the strong model compared to simply mimicking an individual teacher. It confirms that W2SG is more likely to emerge when the student model matches its posterior mean teacher. This aligns with prior work [Agrawal et al., 2024; Sang et al., 2024; Liu and Alahi, 2024; Cui et al., 2025] where multiple teachers collectively train a student model. Our empirical finding holds across different model capacities (ranging from GPT2-Medium to GPT2-XL) and diverse datasets, thereby providing strong support for our theory.

Stronger student reduces population risk. We find that increasing the student model’s complexity leads to lower population risk, demonstrating that more capable models enhance W2SG. It is consistent with the insights in Theorem 4.1 and Remark 4.2.

Bias and variance analysis in W2SG. Notably, scaling up student capacity primarily reduces bias. While both bias and variance decrease, the variance and its reduction remain significantly smaller than bias terms. This differs from Dong et al. [2025], which mainly focuses on variance-dominated scenarios. Moreover, these trends align with Chen et al. [2024], which shows that the trends of bias and variance are consistent, and the variance is upper bounded by the bias. Model ensembles decrease test loss mainly through variance reduction, as incorporating more weak teachers helps mitigate randomness in their outputs.

RCE vs. CE To systematically investigate the role of forward (in Eq. (4)) and reverse (in Eq. (5)) misfit in W2SG training, we conduct a set of experiments comparing the performance of using RCE loss versus CE loss during strong model training. Specifically, we apply the label-proportional smoothing strategy in Proposition 2. A smaller smooth factor α leads to higher predictive uncertainty in the shifted pseudo-labels. When $\alpha = 0$, the predicted distribution will be uniform. The performance of strong model using this label smoothing strategy is shown in Figure 2. We observe that even when $\alpha = 0.001$, where the pseudo-labels are nearly uniform, RCE maintains stable performance without significant degradation. This aligns with Proposition 2. Moreover, in some cases, moderate label shifting even improves accuracy. In contrast, the performance of CE drops rapidly as α decreases. We further empirically study standard knowledge distillation settings as well as KL and reverse KL objectives. More results are provided in Appendix E.

Moreover, the results of Proposition 2 and Figure 2 indicate that RCE might be more suitable for low-confidence samples. Therefore, a combination of CE and RCE may better exploit the information within weak supervision. To explore this idea, we propose confidence-adaptive cross entropy (CACE) loss as: $\mathcal{L}_{\text{CACE}}(y, \hat{y}) = \mathbb{I}(y, c) \cdot \text{RCE}(y, \hat{y}) + (1 - \mathbb{I}(y, c)) \cdot \text{CE}(y, \hat{y})$, where c is the confidence threshold, and $\mathbb{I}(y, c)$ is an indicator function that activates when the soft label y is below c . We also note that the symmetric cross entropy loss (SL) [Wang et al., 2019] shares a similar design philosophy with ours, defined as: $\mathcal{L}_{\text{SL}}(y, \hat{y}) = \lambda_1 \text{RCE}(y, \hat{y}) + \lambda_2 \text{CE}(y, \hat{y})$. Additionally, we compare our method with the auxiliary confidence loss (AUX, defined in Eq. (9)) introduced by Burns et al. [2023].

As shown in Table 1, on simpler datasets like CAI-Harmless, the pseudo labels tend to have higher confidence, where RCE offers no significant advantage over CE. Conversely, on more challenging datasets like HH-RLHF, the lower confidence makes RCE preferable to CE. In both cases, CACE or SL consistently outperforms other three losses. While AUX improves student confidence by adding a regularization term, it requires careful hyperparameter tuning for the warm-up phase. In contrast, CACE and SL leverage the strengths of CE and RCE based on the weak label confidence, without relying on the capacity of student models.

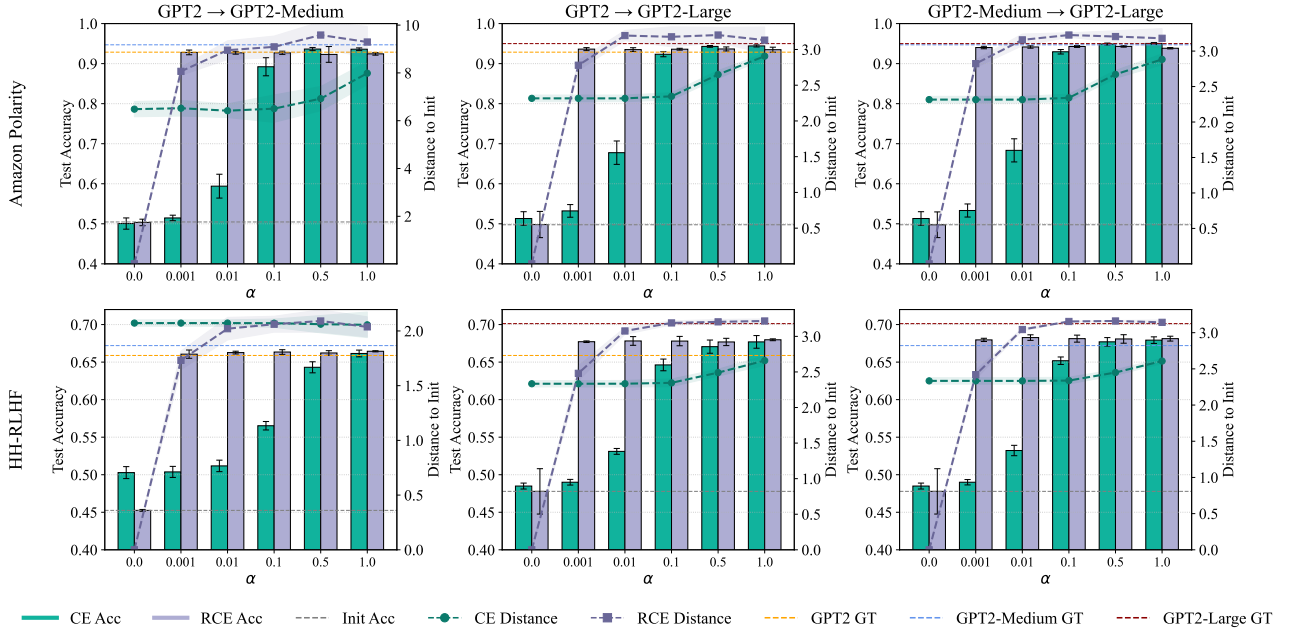


Figure 2: Performance of the GPT2 series models across two datasets under varying α values, comparing CE and RCE losses. “GPT2 \rightarrow GPT2-Medium” denotes GPT2 supervising GPT2-Medium. Left y-axis shows test accuracy, corresponding to the bar plots for CE Acc and RCE Acc. Right y-axis illustrates the L_2 norm between the fine-tuned and initial models, represented by the line plots for CE Distance and RCE Distance. The cases $\alpha = 0$ and $\alpha = 1$ represent uniform and unshifted pseudo-labels, respectively. GT denotes the test accuracy achieved by training with ground truth labels. All experiments are repeated three times.

Table 1: Test accuracy (%) of five loss functions on CAI-Harmless and HH-RLHF datasets. The optimal and suboptimal results are marked in **bold** and underline, respectively. “GPT2 \rightarrow GPT2-Medium” denotes GPT2 supervising GPT2-Medium. All experiments are repeated three times.

Dataset	Model	CE	RCE	AUX	CACE	SL
CAI-Harmless	GPT2 \rightarrow GPT2-Medium	93.05	93.00	92.81	93.44	<u>93.32</u>
	GPT2 \rightarrow GPT2-Large	93.88	94.55	94.51	94.78	<u>94.63</u>
	GPT2-Medium \rightarrow GPT2-Large	95.47	95.40	95.40	95.62	<u>95.58</u>
HH-RLHF	GPT2 \rightarrow GPT2-Medium	66.15	<u>66.44</u>	66.21	66.18	66.65
	GPT2 \rightarrow GPT2-Large	67.69	67.97	67.73	<u>67.82</u>	67.97
	GPT2-Medium \rightarrow GPT2-Large	67.93	68.13	68.08	<u>68.11</u>	68.53

7 Conclusion and Limitations

This work provides a theoretical framework for understanding W2SG through a bias-variance decomposition of Bregman divergence, demonstrating that the student model’s performance gain arises from the expected misfit with the teacher and is enhanced when the student approximates the posterior mean teacher. Our analysis relaxes restrictive assumptions like convexity and highlights the benefits of RCE for handling uncertain supervision. However, some theoretical insights are primarily validated in ridge regression, and the practical scalability of RCE to more complex tasks remains to be explored. Future work could address these limitations by extending the framework to broader architectures and real-world applications.

References

- Ben Adlam, Neha Gupta, Zelda Mariet, and Jamie Smith. Understanding the bias-variance tradeoff of bregman divergences. *arXiv preprint arXiv:2202.04167*, 2022.
- Aakriti Agrawal, Mucong Ding, Zora Che, Chenghao Deng, Anirudh Satheesh, John Langford, and Furong Huang. Ensemw2s: Can an ensemble of llms be leveraged to obtain a stronger llm? *arXiv preprint arXiv:2410.04571*, 2024.
- Jimmy Ba, Murat Erdogdu, Taiji Suzuki, Denny Wu, and Tianzong Zhang. Generalization of two-layer neural networks: An asymptotic viewpoint. In *International Conference on Learning Representations*, 2020. URL <https://openreview.net/forum?id=H1gBsgBYwH>.
- Yuntao Bai, Andy Jones, Kamal Ndousse, Amanda Askell, Anna Chen, Nova DasSarma, Dawn Drain, Stanislav Fort, Deep Ganguli, Tom Henighan, et al. Training a helpful and harmless assistant with reinforcement learning from human feedback. *arXiv preprint arXiv:2204.05862*, 2022a.
- Yuntao Bai, Saurav Kadavath, Sandipan Kundu, Amanda Askell, Jackson Kernion, Andy Jones, Anna Chen, Anna Goldie, Azalia Mirhoseini, Cameron McKinnon, et al. Constitutional ai: Harmlessness from ai feedback, 2022. *arXiv preprint arXiv:2212.08073*, 8(3), 2022b.
- Arindam Banerjee, Srujana Merugu, Inderjit S Dhillon, and Joydeep Ghosh. Clustering with bregman divergences. *Journal of machine learning research*, 6(Oct):1705–1749, 2005.
- Mikhail Belkin, Daniel Hsu, Siyuan Ma, and Soumik Mandal. Reconciling modern machine-learning practice and the classical bias–variance trade-off. *Proceedings of the National Academy of Sciences*, 116(32):15849–15854, 2019.
- Lev M Bregman. The relaxation method of finding the common point of convex sets and its application to the solution of problems in convex programming. *USSR computational mathematics and mathematical physics*, 7(3):200–217, 1967.
- Collin Burns, Pavel Izmailov, Jan Hendrik Kirchner, Bowen Baker, Leo Gao, Leopold Aschenbrenner, Yining Chen, Adrien Ecoffet, Manas Joglekar, Jan Leike, et al. Weak-to-strong generalization: Eliciting strong capabilities with weak supervision. *arXiv preprint arXiv:2312.09390*, 2023.
- Moses Charikar, Chirag Pabbaraju, and Kirankumar Shiragur. Quantifying the gain in weak-to-strong generalization. *Advances in neural information processing systems*, 2024.
- Gong Chen and Marc Teboulle. Convergence analysis of a proximal-like minimization algorithm using bregman functions. *SIAM Journal on Optimization*, 3(3):538–543, 1993.
- Lin Chen, Michal Lukasik, Wittawat Jitkittum, Chong You, and Sanjiv Kumar. On bias-variance alignment in deep models. In *The Twelfth International Conference on Learning Representations*, 2024. URL <https://openreview.net/forum?id=i2Phucne30>.
- Ziyun Cui, Ziyang Zhang, Guangzhi Sun, Wen Wu, and Chao Zhang. Bayesian weak-to-strong from text classification to generation. In *The Thirteenth International Conference on Learning Representations*, 2025.
- James Demmel. The componentwise distance to the nearest singular matrix. *SIAM Journal on Matrix Analysis and Applications*, 13(1):10–19, 1992.
- Thomas G Dietterich. Ensemble methods in machine learning. In *International workshop on multiple classifier systems*, pages 1–15. Springer, 2000.
- Yijun Dong, Yicheng Li, Yunai Li, Jason D Lee, and Qi Lei. Discrepancies are virtue: Weak-to-strong generalization through lens of intrinsic dimension. *arXiv preprint arXiv:2502.05075*, 2025.
- Shashwat Goel, Joschka Struber, Ilze Amanda Auzina, Karuna K Chandra, Ponnurangam Kumaraguru, Douwe Kiela, Ameya Prabhu, Matthias Bethge, and Jonas Geiping. Great models think alike and this undermines ai oversight. *arXiv preprint arXiv:2502.04313*, 2025.
- Jianyuan Guo, Hanling Chen, Chengcheng Wang, Kai Han, Chang Xu, and Yunhe Wang. Vision superalignment: Weak-to-strong generalization for vision foundation models. *arXiv preprint arXiv:2402.03749*, 2024.

- Trevor Hastie, Andrea Montanari, Saharon Rosset, and Ryan J Tibshirani. Surprises in high-dimensional ridgeless least squares interpolation. *Annals of statistics*, 50(2):949, 2022.
- Geoffrey Hinton, Oriol Vinyals, and Jeff Dean. Distilling the knowledge in a neural network. *arXiv preprint arXiv:1503.02531*, 2015.
- Muhammed Emrullah Ildiz, Halil Alperen Gozeten, Ege Onur Taga, Marco Mondelli, and Samet Oymak. High-dimensional analysis of knowledge distillation: Weak-to-strong generalization and scaling laws. In *The Thirteenth International Conference on Learning Representations*, 2025.
- Hao Lang, Fei Huang, and Yongbin Li. Debate helps weak-to-strong generalization. *arXiv preprint arXiv:2501.13124*, 2025.
- Hunter Lang, David Sontag, and Aravindan Vijayaraghavan. Theoretical analysis of weak-to-strong generalization. In *The Thirty-eighth Annual Conference on Neural Information Processing Systems*, 2024.
- Yuejiang Liu and Alexandre Alahi. Co-supervised learning: Improving weak-to-strong generalization with hierarchical mixture of experts. *arXiv preprint arXiv:2402.15505*, 2024.
- Zhuang Liu, Zhiqiu Xu, Joseph Jin, Zhiqiang Shen, and Trevor Darrell. Dropout reduces underfitting. In *International Conference on Machine Learning*, pages 22233–22248. PMLR, 2023.
- Yougang Lyu, Lingyong Yan, Zihan Wang, Dawei Yin, Pengjie Ren, Maarten de Rijke, and Zhaochun Ren. Macpo: Weak-to-strong alignment via multi-agent contrastive preference optimization. In *The Thirteenth International Conference on Learning Representations*, 2025.
- Vladimir A Marčenko and Leonid Andreevich Pastur. Distribution of eigenvalues for some sets of random matrices. *Mathematics of the USSR-Sbornik*, 1(4):457, 1967.
- Julian McAuley and Jure Leskovec. Hidden factors and hidden topics: understanding rating dimensions with review text. In *Proceedings of the 7th ACM conference on Recommender systems*, pages 165–172, 2013.
- Marko Medvedev, Kaifeng Lyu, Dingli Yu, Sanjeev Arora, Zhiyuan Li, and Nathan Srebro. Weak-to-strong generalization even in random feature networks, provably. *arXiv preprint arXiv:2503.02877*, 2025.
- Song Mei and Andrea Montanari. The generalization error of random features regression: Precise asymptotics and the double descent curve. *Communications on Pure and Applied Mathematics*, 75(4):667–766, 2022.
- Tom Minka et al. Divergence measures and message passing. Technical report, Microsoft Research, 2005.
- Abhijeet Mulgund and Chirag Pabbaraju. Relating misfit to gain in weak-to-strong generalization beyond the squared loss. *arXiv preprint arXiv:2501.19105*, 2025.
- Preetum Nakkiran, Gal Kaplun, Yamini Bansal, Tristan Yang, Boaz Barak, and Ilya Sutskever. Deep double descent: Where bigger models and more data hurt. In *International Conference on Learning Representations*, 2020. URL <https://openreview.net/forum?id=B1g5sA4twr>.
- OpenAI. Introducing superalignment, 2023. URL <https://openai.com/index/introducing-superalignment/>.
- Martin Pawelczyk, Lillian Sun, Zhenting Qi, Aounon Kumar, and Himabindu Lakkaraju. Generalizing trust: Weak-to-strong trustworthiness in language models. *arXiv preprint arXiv:2501.00418*, 2024.
- David Pfau. A generalized bias-variance decomposition for bregman divergences. *Unpublished manuscript*, 2013.
- Alec Radford, Jeffrey Wu, Rewon Child, David Luan, Dario Amodei, Ilya Sutskever, et al. Language models are unsupervised multitask learners. *OpenAI blog*, 1(8):9, 2019.
- Jitao Sang, Yuhang Wang, Jing Zhang, Yanxu Zhu, Chao Kong, Junhong Ye, Shuyu Wei, and Jinlin Xiao. Improving weak-to-strong generalization with scalable oversight and ensemble learning. *arXiv preprint arXiv:2402.00667*, 2024.
- Changho Shin, John Cooper, and Frederic Sala. Weak-to-strong generalization through the data-centric lens. In *The Thirteenth International Conference on Learning Representations*, 2025.

- Seamus Somerstep, Felipe Maia Polo, Moulinath Banerjee, Yaacov Ritov, Mikhail Yurochkin, and Yuekai Sun. A transfer learning framework for weak to strong generalization. In *The Thirteenth International Conference on Learning Representations*, 2025.
- Martin J Wainwright. *High-dimensional statistics: A non-asymptotic viewpoint*, volume 48. Cambridge university press, 2019.
- Yisen Wang, Xingjun Ma, Zaiyi Chen, Yuan Luo, Jinfeng Yi, and James Bailey. Symmetric cross entropy for robust learning with noisy labels. In *Proceedings of the IEEE/CVF international conference on computer vision*, pages 322–330, 2019.
- Johannes Welbl, Nelson F Liu, and Matt Gardner. Crowdsourcing multiple choice science questions. *arXiv preprint arXiv:1707.06209*, 2017.
- David X Wu and Anant Sahai. Provable weak-to-strong generalization via benign overfitting. In *The Thirteenth International Conference on Learning Representations*, 2025.
- Yihao Xue, Jiping Li, and Baharan Mirzasoleiman. Representations shape weak-to-strong generalization: Theoretical insights and empirical predictions. *arXiv preprint arXiv:2502.00620*, 2025.
- Wenkai Yang, Shiqi Shen, Guangyao Shen, Wei Yao, Yong Liu, Zhi Gong, Yankai Lin, and Ji-Rong Wen. Super (ficial)-alignment: Strong models may deceive weak models in weak-to-strong generalization. In *The Thirteenth International Conference on Learning Representations*, 2025.
- Yuqing Yang, Yan Ma, and Pengfei Liu. Weak-to-strong reasoning. In *Findings of the Association for Computational Linguistics: EMNLP 2024*, pages 8350–8367, 2024.
- Zitong Yang, Yaodong Yu, Chong You, Jacob Steinhardt, and Yi Ma. Rethinking bias-variance trade-off for generalization of neural networks. In *International Conference on Machine Learning*, pages 10767–10777. PMLR, 2020.
- Wei Yao, Wenkai Yang, Ziqiao Wang, Yankai Lin, and Yong Liu. Revisiting weak-to-strong generalization in theory and practice: Reverse kl vs. forward kl. *arXiv preprint arXiv:2502.11107*, 2025a.
- Wei Yao, Wenkai Yang, Ziqiao Wang, Yankai Lin, and Yong Liu. Understanding the capabilities and limitations of weak-to-strong generalization. *arXiv preprint arXiv:2502.01458*, 2025b.
- Yaowen Ye, Cassidy Laidlaw, and Jacob Steinhardt. Iterative label refinement matters more than preference optimization under weak supervision. In *The Thirteenth International Conference on Learning Representations*, 2025.
- Yucheng Zhou, Jianbing Shen, and Yu Cheng. Weak to strong generalization for large language models with multi-capabilities. In *The Thirteenth International Conference on Learning Representations*, 2025.
- Zhi-Hua Zhou. *Ensemble methods: foundations and algorithms*. CRC press, 2025.

Content

A Previous Misfit-based Results	14
B Omitted Proofs in Section 3 and Additional Results	15
B.1 Proof of Theorem 3.1	15
B.2 Additional Result: Expected Misfit for Arbitrary Two Models	16
B.3 Proof of Corollary 3.1	17
C Omitted Proofs in Section 4	18
C.1 Proof of Corollary 4.1	18
C.2 Proof of Theorem 4.1	18
C.3 Monotonicity Analysis	20
D Omitted Proofs in Section 5	20
D.1 Proof of Corollary 5.1	20
D.2 Proof of Proposition 1	21
D.3 Proof of Proposition 2	21
D.4 Gradient Analysis	23
E Experimental Details and Additional Results	23
E.1 Experimental Details	23
E.2 Bias and Variance Estimation in W2SG	24
E.3 Additional Empirical Validation of RCE’s Robustness to Predictive Uncertainty	25

Appendix

A Previous Misfit-based Results

Theorem A.1 (Restatement of Theorem 1 from Charikar et al. [2024]). *This Theorem considers the squared loss as a special case of Bregman divergence $D_\phi(\cdot, \cdot)$, i.e., $\phi(x) = \|x\|^2$. Let $h_s : \mathbb{R}^d \rightarrow \mathbb{R}^{d_s}$ and $h_w : \mathbb{R}^d \rightarrow \mathbb{R}^{d_w}$ be the strong and weak model representation maps respectively. Given some data labeled by g , let $f_w \circ h_w$ be the function learnt by the weak model, for some classifier head $f_w : \mathbb{R}^{d_w} \rightarrow \mathbb{R}$. For a convex set of functions \mathcal{F}_s mapping \mathbb{R}^{d_s} to \mathbb{R} let*

$$f_{sw} = \operatorname{argmin}_{f \in \mathcal{F}_s} \mathbb{E}_X \|f(h_s(X)) - f_w(h_w(X))\|^2,$$

be the function learnt by the strong model under weak supervision. Lastly, let us assume that there exists $f_s \in \mathcal{F}_s$ such that $f_s \circ h_s = g$. Then, we have that

$$\mathbb{E}_X \|f_{sw}(h_s(X)) - g(X)\|^2 \leq \mathbb{E}_X \|f_w(h_w(X)) - g(X)\|^2 - \mathbb{E}_X \|f_{sw}(h_s(X)) f_w(h_w(X))\|^2. \quad (10)$$

Remark A.1. *In comparison, our bound in Corollary 4.1 is*

$$\mathbb{E}_{X, W'} \|g(X) - f_{W'}(X)\|^2 \leq \mathbb{E}_{X, W'} \|g(X) - f_W(X)\|^2 - \mathbb{E}_{X, W', W} \|f_{W'}(X) - f_W(X)\|^2 + \epsilon_2,$$

Our bound differs from Theorem A.1 in that it focuses on the expected population risk, that is, the expectation is taken over both the data distribution and the model parameters. As mentioned in the main text, this enables us to remove the convexity assumption by invoking Lemma 2.1. Notably, when restricted to convex function classes, our result recovers Theorem A.1, as convexity guarantees the last term $\mathbb{E}_{W'} \langle \mathbb{E}_{W|W'} [f_W^(x)] - f_{W'}^*(x), g(x) - f_{W'}(x) \rangle \leq 0$ in Eq. (16) in our framework, following similar developments as those in Charikar et al. [2024]. This recovery can also be seen by comparing [Charikar et al., 2024, Eq. (8)] with our Eq. (16). Specifically, taking expectations over both $(W, W') \sim P_{W, W'}$ in their bound obtains a result similar to ours, corresponding to a non-positive residual term in Eq. (16) in our proof.*

Theorem A.2 (Restatement of Theorem 4.1 from Mulgund and Pabbaraju [2025]). *Let ϕ be a proper convex function as defined in Definition 2.1. Let h_s, h_w be defined in the same way in Theorem A.1. Let $f_w : \mathbb{R}^{d_w} \rightarrow \mathcal{Y}$ be the weak model finetune layer, and $g : \mathcal{X} \rightarrow \mathcal{Y}$ be the target function. Let \mathcal{F} be a class of functions mapping $\mathbb{R}^{d_s} \rightarrow \mathcal{Y}$. If the following hold:*

1. (Realizability) $\exists f_* \in \mathcal{F}$ s.t. $g = f_* \circ h_s$,
2. (Convexity) \mathcal{F} is a convex set of functions,
3. (Sequential Consistency) For $y \in \mathcal{Y}$ fixed, if $D_\phi(x_n, y) \rightarrow 0$, then $x_n \rightarrow y$,

then for any $\epsilon > 0$, there exists $\delta > 0$ such that for all $f_s \in \mathcal{F}$ that satisfy

$$\mathbb{E}_X [D_\phi(f_s(h_s(X)), f_w(h_w(X)))] \leq \inf_{f \in \mathcal{F}} \mathbb{E}_X [D_\phi(f(h_s(X)), f_w(h_w(X)))] + \delta,$$

we have

$$\mathbb{E}_X [D_\phi(g(X), f_s(h_s(X)))] \leq \mathbb{E}_X [D_\phi(g(X), f_w(h_w(X)))] - \mathbb{E}_X [D_\phi(f_s(h_s(X)), f_w(h_w(X)))] + \epsilon. \quad (11)$$

Remark A.2. *In contrast to Theorem A.2, our bounds in Theorem 3.1 are derived without relying on any of the three assumptions mentioned earlier: realizability, convexity, and sequential consistency. Moreover, the conditions under which the remainder term ϵ vanishes differ between Eq. (11) and Eq. (4). Specifically, in the case of Eq. (11), the ϵ term disappears when the student model satisfies*

$$f_s = \arg \min_{f \in \mathcal{F}} \mathbb{E}_X [D_\phi(f(h_s(X)), f_w(h_w(X)))].$$

By contrast, the ϵ_1 term in Eq. (4) vanishes under the condition that the student model is close to its posterior mean teacher, as established in our theoretical analysis.

B Omitted Proofs in Section 3 and Additional Results

B.1 Proof of Theorem 3.1

Theorem 3.1 is restated as follows.

Theorem 3.1. *Under the teacher-student setting, the following inequalities hold,*

$$\mathbb{E} [\mathcal{D}_\phi (g(X), f_{W'}(X))] \leq \mathbb{E} [\mathcal{D}_\phi (g(X), f_W(X))] - \mathbb{E} [\mathcal{D}_\phi (f_{W'}(X), f_W(X))] + \epsilon_1, \quad (4)$$

$$\mathbb{E} [\mathcal{D}_\phi (f_{W'}(X), g(X))] \leq \mathbb{E} [\mathcal{D}_\phi (f_W(X), g(X))] - \mathbb{E} [\mathcal{D}_\phi (f_W(X), f_{W'}(X))] + \epsilon_2, \quad (5)$$

where

$$\begin{aligned} \epsilon_1 &= \sqrt{\mathbb{E} \|f_{W'}^*(X) - \mathbb{E} [f_W^*(X) | W', X]\|^2} \sqrt{\mathbb{E} \|g(X) - f_{W'}(X)\|^2}, \\ \epsilon_2 &= \sqrt{\mathbb{E} \|f_{W'}(X) - \mathbb{E} [f_W(X) | W', X]\|^2} \sqrt{\mathbb{E} \|g^*(X) - f_{W'}^*(X)\|^2}. \end{aligned}$$

Proof. We first prove Eq. (4).

For any given test instance x and a fixed student model $f_{w'}$, by Eq. (3), we have the following conditional bias-variance decomposition for the weak teacher model,

$$\mathbb{E}_{W|w'} [\mathcal{D}_\phi (g(x), f_W(x))] = \mathcal{D}_\phi (g(x), \mathcal{E}_{W|w'} [f_W(x)]) + \mathbb{E}_{W|w'} [\mathcal{D}_\phi (\mathcal{E}_{W|w'} [f_W(x)], f_W(x))]. \quad (12)$$

Similarly, we also have

$$\mathbb{E}_{W|w'} [\mathcal{D}_\phi (f_{w'}(x), f_W(x))] = \mathcal{D}_\phi (f_{w'}(x), \mathcal{E}_{W|w'} [f_W(x)]) + \mathbb{E}_{W|w'} [\mathcal{D}_\phi (\mathcal{E}_{W|w'} [f_W(x)], f_W(x))]. \quad (13)$$

Notice that both Eq. (12) and Eq. (13) contain the conditional dual variance term of weak model, namely $\mathbb{E}_{W|w'} [\mathcal{D}_\phi (\mathcal{E}_{W|w'} [f_W(x)], f_W(x))]$, so combining these two equations give us

$$\begin{aligned} &\mathcal{D}_\phi (g(x), \mathcal{E}_{W|w'} [f_W(x)]) \\ &= \mathbb{E}_{W|w'} [\mathcal{D}_\phi (g(x), f_W(x))] - \mathbb{E}_{W|w'} [\mathcal{D}_\phi (f_{w'}(x), f_W(x))] + \mathcal{D}_\phi (f_{w'}(x), \mathcal{E}_{W|w'} [f_W(x)]). \end{aligned}$$

Then, by taking expectation over W' for both sides, we obtain

$$\begin{aligned} &\mathbb{E}_{W'} [\mathcal{D}_\phi (g(x), \mathcal{E}_{W|W'} [f_W(x)])] \\ &= \mathbb{E}_W [\mathcal{D}_\phi (g(x), f_W(x))] - \mathbb{E}_{W',W} [\mathcal{D}_\phi (f_{W'}(x), f_W(x))] + \mathbb{E}_{W'} [\mathcal{D}_\phi (f_{W'}(x), \mathcal{E}_{W|W'} [f_W(x)])]. \end{aligned} \quad (14)$$

We now further decompose the LHS in Eq. (14) by invoking Eq. (1) here,.

$$\begin{aligned} \mathbb{E}_{W'} [\mathcal{D}_\phi (g(x), \mathcal{E}_{W|W'} [f_W(x)])] &= \mathbb{E}_{W'} [\mathcal{D}_\phi (g(x), f_{W'}(x))] + \mathbb{E}_{W'} [\mathcal{D}_\phi (f_{W'}(x), \mathcal{E}_{W|W'} [f_W(x)])] \\ &\quad - \mathbb{E}_{W'} \langle \mathbb{E}_{W|W'} [f_W^*(x)] - f_{W'}^*(x), g(x) - f_{W'}(x) \rangle. \end{aligned} \quad (15)$$

Plugging Eq. (15) into Eq. (14), taking expectation over X for both sides and re-arranging terms, we have

$$\begin{aligned} &\mathbb{E}_{X,W'} [\mathcal{D}_\phi (g(X), f_{W'}(X))] \\ &= \mathbb{E}_{X,W} [\mathcal{D}_\phi (g(X), f_W(X))] - \mathbb{E}_{X,W',W} [\mathcal{D}_\phi (f_{W'}(X), f_W(X))] \\ &\quad + \mathbb{E}_{X,W'} \langle \mathbb{E}_{W|W'} [f_W^*(X)] - f_{W'}^*(X), g(X) - f_{W'}(X) \rangle \end{aligned} \quad (16)$$

$$\begin{aligned} &\leq \mathbb{E}_{X,W} [\mathcal{D}_\phi (g(X), f_W(X))] - \mathbb{E}_{X,W',W} [\mathcal{D}_\phi (f_{W'}(X), f_W(X))] \\ &\quad + \sqrt{(\mathbb{E}_{X,W'} \langle \mathbb{E}_{W|W'} [f_W^*(X)] - f_{W'}^*(X), g(X) - f_{W'}(X) \rangle)^2} \\ &\leq \mathbb{E}_{X,W} [\mathcal{D}_\phi (g(X), f_W(X))] - \mathbb{E}_{X,W',W} [\mathcal{D}_\phi (f_{W'}(X), f_W(X))] \\ &\quad + \sqrt{\mathbb{E}_{X,W'} \|\mathbb{E}_{W|W'} [f_W^*(X)] - f_{W'}^*(X)\|^2} \sqrt{\mathbb{E}_{X,W'} \|g(X) - f_{W'}(X)\|^2}, \end{aligned} \quad (17)$$

where the last inequality is by Cauchy-Schwarz inequality. Hence, the first inequality in the theorem has been proved.

The second inequality, namely Eq. (5), can be proved by following the same developments. Similar to Eq. (14), it's easy to see that we also have

$$\begin{aligned} &\mathbb{E}_{W'} [\mathcal{D}_\phi (\mathbb{E}_{W|W'} [f_W(x)], g(x))] \\ &= \mathbb{E}_W [\mathcal{D}_\phi (f_W(x), g(x))] - \mathbb{E}_{W',W} [\mathcal{D}_\phi (f_W(x), f_{W'}(x))] + \mathbb{E}_{W'} [\mathcal{D}_\phi (\mathbb{E}_{W|W'} [f_W(x)], f_{W'}(x))]. \end{aligned}$$

We then decompose the LHS above by using Eq. (1),

$$\begin{aligned}\mathbb{E}_{W'} [\mathcal{D}_\phi (\mathbb{E}_{W|W'} [f_W(x)], g(x))] &= \mathbb{E}_{W'} [\mathcal{D}_\phi (\mathbb{E}_{W|W'} [f_W(x)], f_{W'}(x))] + \mathbb{E}_{W'} [\mathcal{D}_\phi (f_{W'}(x), g(x))] \\ &\quad - \mathbb{E}_{W'} \langle g^*(x) - f_{W'}^*(x), \mathbb{E}_{W|W'} [f_W(x)] - f_{W'}(x) \rangle.\end{aligned}$$

Consequently, we have

$$\begin{aligned}&\mathbb{E}_{X,W'} [\mathcal{D}_\phi (f_{W'}(X), g(X))] \\ &= \mathbb{E}_{X,W} [\mathcal{D}_\phi (f_W(X), g(X))] - \mathbb{E}_{X,W',W} [\mathcal{D}_\phi (f_W(X), f_{W'}(X))] \\ &\quad + \mathbb{E}_{X,W'} \langle g^*(X) - f_{W'}^*(X), \mathbb{E}_{W|W'} [f_W(X)] - f_{W'}(X) \rangle \\ &\leq \mathbb{E}_{X,W} [\mathcal{D}_\phi (f_W(X), g(X))] - \mathbb{E}_{X,W',W} [\mathcal{D}_\phi (f_W(X), f_{W'}(X))] \\ &\quad + \sqrt{\mathbb{E}_{X,W'} \|g^*(X) - f_{W'}^*(X)\|^2} \sqrt{\mathbb{E}_{X,W'} \|f_{W'}(X) - \mathbb{E}_{W|W'} [f_W(X)]\|^2}.\end{aligned}\tag{18}$$

This completes the proof. \square

B.2 Additional Result: Expected Misfit for Arbitrary Two Models

Theorem B.1. *For arbitrary two models f_w and $f_{w'}$, the following inequalities hold for any Bregman divergence,*

$$\mathbb{E}_{W'} [\mathcal{D}_\phi (g(X), f_{W'}(X))] \leq \mathbb{E}_W [\mathcal{D}_\phi (g(X), f_W(X))] - \mathbb{E}_{P_X P_{W'}, P_W} [\mathcal{D}_\phi (f_{W'}(X), f_W(X))] + \epsilon_1,\tag{19}$$

$$\mathbb{E}_{W'} [\mathcal{D}_\phi (f_{W'}(X), g(X))] \leq \mathbb{E}_W [\mathcal{D}_\phi (f_W(X), g(X))] - \mathbb{E}_{P_X P_{W'}, P_W} [\mathcal{D}_\phi (f_W(X), f_{W'}(X))] + \epsilon_2,\tag{20}$$

where

$$\begin{aligned}\epsilon_1 &= \sqrt{\mathbb{E}_{W'} \|f_{W'}^*(X) - \mathbb{E}_W [f_W^*(X)]\|^2} \sqrt{\mathbb{E} \|g(X) - f_{W'}(X)\|^2}, \\ \epsilon_2 &= \sqrt{\mathbb{E}_{W'} \|f_{W'}(X) - \mathbb{E}_W [f_W(X)]\|^2} \sqrt{\mathbb{E}_{W'} \|g^*(X) - f_{W'}^*(X)\|^2}.\end{aligned}$$

Remark B.1. *Note that, unlike Theorem 3.1, the misfit terms in Theorem B.1 are defined under the expectation with respect to the product of the marginal distributions of the teacher and student models, i.e., $(W, W') \sim P_W P_{W'}$. In contrast, Theorem 3.1 considers the joint distribution $(W, W') \sim P_{W, W'}$, thereby capturing potential dependencies between the models. As a result, Theorem B.1 completely ignores any such dependencies, making it applicable even when the teacher and student models are independently drawn. Additionally, the conditions under which the remainder terms ϵ_1 and ϵ_2 vanish are now characterized by the student model being sufficiently close to the expected teacher model (or the dual expected teacher). Finally, observe that in Theorem B.1, the misfit terms remain nonzero even when $P_{W'}$ is the same P_W as W' is treated as an independent copy of W in this case.*

Proof of Theorem B.1. We first prove the first inequality, i.e. Eq. (19).

For any given test instance x and a fixed student model $f_{w'}$, by Eq. (3), we have the following bias-variance decomposition for the weak teacher model,

$$\mathbb{E}_W [\mathcal{D}_\phi (g(x), f_W(x))] = \mathcal{D}_\phi (g(x), \mathcal{E}_W [f_W(x)]) + \mathbb{E}_W [\mathcal{D}_\phi (\mathcal{E}_W [f_W(x)], f_W(x))].\tag{21}$$

Similarly, for the same x and the student model $f_{w'}$, we also have

$$\mathbb{E}_W [\mathcal{D}_\phi (f_{w'}(x), f_W(x))] = \mathcal{D}_\phi (f_{w'}(x), \mathcal{E}_W [f_W(x)]) + \mathbb{E}_W [\mathcal{D}_\phi (\mathcal{E}_W [f_W(x)], f_W(x))].\tag{22}$$

Both Eq. (21) and Eq. (22) contain the dual variance term of weak model, namely $\mathbb{E}_W [\mathcal{D}_\phi (\mathcal{E}_W [f_W(x)], f_W(x))]$, so combining these two equations give us

$$\begin{aligned}\mathcal{D}_\phi (g(x), \mathcal{E}_W [f_W(x)]) &= \mathbb{E}_W [\mathcal{D}_\phi (g(x), f_W(x))] - \mathbb{E}_W [\mathcal{D}_\phi (f_{w'}(x), f_W(x))] \\ &\quad + \mathcal{D}_\phi (f_{w'}(x), \mathcal{E}_W [f_W(x)]).\end{aligned}\tag{23}$$

We now further decompose the LHS above by invoking Eq. (1) here.

$$\begin{aligned}\mathcal{D}_\phi (g(x), \mathcal{E}_W [f_W(x)]) &= \mathcal{D}_\phi (g(x), f_{w'}(x)) + \mathcal{D}_\phi (f_{w'}(x), \mathcal{E}_W [f_W(x)]) \\ &\quad - \langle \mathbb{E}_W [f_W^*(x)] - f_{w'}^*(x), g(x) - f_{w'}(x) \rangle.\end{aligned}\tag{24}$$

Then, by plugging Eq. (24) into Eq. (23), canceling the term $D_\phi(f_{w'}(x), \mathcal{E}_W[f_W(x)])$ and taking expectation over W', X for both sides, we obtain

$$\begin{aligned}
& \mathbb{E}_{X,W'} [D_\phi(g(X), f_{W'}(X))] \\
&= \mathbb{E}_{X,W} [D_\phi(g(X), f_W(X))] - \mathbb{E}_{X,W',W} [D_\phi(f_{W'}(X), f_W(X))] \\
&\quad + \mathbb{E}_{X,W'} \langle \mathbb{E}_W[f_W^*(X)] - f_{W'}^*(X), g(X) - f_{W'}(X) \rangle \\
&\leq \mathbb{E}_{X,W} [D_\phi(g(X), f_W(X))] - \mathbb{E}_{X,W',W} [D_\phi(f_{W'}(X), f_W(X))] \\
&\quad + \sqrt{(\mathbb{E}_{X,W'} \langle \mathbb{E}_W[f_W^*(X)] - f_{W'}^*(X), g(X) - f_{W'}(X) \rangle)^2} \\
&\leq \mathbb{E}_{X,W} [D_\phi(g(X), f_W(X))] - \mathbb{E}_{X,W',W} [D_\phi(f_{W'}(X), f_W(X))] \\
&\quad + \sqrt{\mathbb{E}_{X,W'} \|\mathbb{E}_W[f_W^*(X)] - f_{W'}^*(X)\|^2} \sqrt{\mathbb{E}_{X,W'} \|g(X) - f_{W'}(X)\|^2}, \tag{25}
\end{aligned}$$

where the last inequality is by Cauchy-Schwarz inequality. Hence, the first inequality in the theorem has been proved.

The second inequality, namely Eq. (20), can be proved by following the same developments. Similar to Eq. (23), it's easy to see that we also have

$$\begin{aligned}
& D_\phi(\mathbb{E}_W[f_W(x)], g(x)) \\
&= \mathbb{E}_W [D_\phi(f_W(x), g(x))] - \mathbb{E}_W [D_\phi(f_W(x), f_{w'}(x))] + D_\phi(\mathbb{E}_W[f_W(x)], f_{w'}(x)).
\end{aligned}$$

We then decompose the LHS above by using Eq. (1),

$$\begin{aligned}
D_\phi(\mathbb{E}_W[f_W(x)], g(x)) &= D_\phi(\mathbb{E}_W[f_W(x)], f_{w'}(x)) + D_\phi(f_{w'}(x), g(x)) \\
&\quad - \langle g^*(x) - f_{w'}^*(x), \mathbb{E}_W[f_W(x)] - f_{w'}(x) \rangle.
\end{aligned}$$

Consequently, we have

$$\begin{aligned}
& \mathbb{E}_{X,W'} [D_\phi(f_{W'}(X), g(X))] \\
&= \mathbb{E}_{X,W} [D_\phi(f_W(X), g(X))] - \mathbb{E}_{X,W',W} [D_\phi(f_W(X), f_{W'}(X))] \\
&\quad + \mathbb{E}_{X,W'} \langle g^*(X) - f_{W'}^*(X), \mathbb{E}_W[f_W(X)] - f_{W'}(X) \rangle \\
&\leq \mathbb{E}_{X,W} [D_\phi(f_W(X), g(X))] - \mathbb{E}_{X,W',W} [D_\phi(f_W(X), f_{W'}(X))] \\
&\quad + \sqrt{\mathbb{E}_{X,W'} \|g^*(X) - f_{W'}^*(X)\|^2} \sqrt{\mathbb{E}_{X,W'} \|f_{W'}(X) - \mathbb{E}_W[f_W(X)]\|^2}. \tag{26}
\end{aligned}$$

This completes the proof. \square

B.3 Proof of Corollary 3.1

We first restate Corollary 3.1 as follows.

Corollary 3.1. *Under the teacher-student setting, if $f_{W'}(x) = \mathcal{E}[f_W(x)|W']$ for $\forall x \in \mathcal{X}$, then*

$$\mathbb{E} [D_\phi(g(X), f_{W'}(X))] = \mathbb{E} [D_\phi(g(X), f_W(X))] - \mathbb{E} [D_\phi(\mathcal{E}[f_W(X)|W', X], f_W(X))]. \tag{6}$$

Furthermore, if $f_{W'}(x) = \mathbb{E}[f_W(x)|W']$ for $\forall x \in \mathcal{X}$, then

$$\mathbb{E} [D_\phi(f_{W'}(X), g(X))] = \mathbb{E} [D_\phi(f_W(X), g(X))] - \mathbb{E} [D_\phi(f_W(X), \mathbb{E}[f_W(X)|W', X])]. \tag{7}$$

Proof. If $f_{W'}(x) = \mathcal{E}[f_W(x)|W']$ for $\forall x \in \mathcal{X}$, then by definition, $f_{W'}^*(x) = \mathbb{E}[f_W(x)|W']$, which directly implies $\epsilon_1 = 0$. Furthermore, since $f_{W'}^*(x) = \mathbb{E}[f_W(x)|W']$, the last term in Eq. (15) becomes zero so there is no need to apply the Cauchy-Schwarz inequality in the proof of Theorem 3.1 to obtain ϵ_1 . Consequently, the following equality holds directly from Theorem 3.1:

$$\mathbb{E}_{X,W'} [D_\phi(g(X), f_{W'}(X))] = \mathbb{E}_{X,W} [D_\phi(g(X), f_W(X))] - \mathbb{E}_{X,W',W} [D_\phi(\mathcal{E}_W[f_W(X)|W', X], f_W(X))].$$

Similarly, if $f_{W'}(x) = \mathbb{E}[f_W(x)|W']$ for $\forall x \in \mathcal{X}$, we obtain the following by analogous reasoning:

$$\mathbb{E}_{X,W'} [D_\phi(f_{W'}(X), g(X))] = \mathbb{E}_{X,W} [D_\phi(f_W(X), g(X))] - \mathbb{E}_{X,W',W} [D_\phi(f_W(X), \mathbb{E}_W[f_W(X)|W', X])]. \tag{27}$$

This completes the proof. \square

C Omitted Proofs in Section 4

C.1 Proof of Corollary 4.1

We first restate Corollary 4.1.

Corollary 4.1. *Let $\phi(x) = \|x\|^2$, then the following inequality holds,*

$$\mathbb{E}\|g(X) - f_{W'}(X)\|^2 \leq \mathbb{E}\|g(X) - f_W(X)\|^2 - \mathbb{E}\|f_{W'}(X) - f_W(X)\|^2 + \epsilon_2,$$

where $\epsilon_2 = 2\sqrt{\mathbb{E}\|f_{W'}(X) - \mathbb{E}[f_{W'}(X) | W', X]\|^2} \sqrt{\mathbb{E}\|g(X) - f_{W'}(X)\|^2}$.

Proof. Let $\phi(x) = \|x\|^2$ so $x^* = \nabla\phi(x) = 2x$ and $D_\phi(x, y) = \|x - y\|^2$. Clearly, we have $\epsilon_1 = \epsilon_2$ and $D_\phi(x, y) = D_\phi(y, x)$ in this case. Then, by Theorem 3.1, it is easy to see that

$$\begin{aligned} \mathbb{E}\|g(X) - f_{W'}(X)\|^2 &\leq \mathbb{E}\|g(X) - f_W(X)\|^2 - \mathbb{E}\|f_{W'}(X) - f_W(X)\|^2 \\ &\quad + 2\sqrt{\mathbb{E}\|f_{W'}(X) - \mathbb{E}[f_{W'}(X) | W', X]\|^2} \sqrt{\mathbb{E}\|g(X) - f_{W'}(X)\|^2}. \end{aligned}$$

This completes the proof. \square

C.2 Proof of Theorem 4.1

We first restate Theorem 4.1.

Theorem 4.1. *Assume $\mathbb{E}\|W\|^2 \leq B$ for some constant $B \in (0, \infty)$, and there exists $\gamma \in (1, \infty)$ s.t. $\frac{d_s}{d_w} \rightarrow \gamma$ as $d_s, d_w \rightarrow \infty$, and $\frac{n}{d_w} \rightarrow \infty$ as $n, d_w \rightarrow \infty$. Let $\eta = \frac{n}{d_w}\eta_0$ for some fixed $\eta_0 > 0$. Then, as $n, d_s, d_w \rightarrow \infty$, the following bound holds a.s.,*

$$\mathbb{E}\|f_{W'}(X) - f_W(X)\|^2 \leq Bh(\eta_0, \gamma),$$

where $h(\eta_0, \gamma) = \frac{\eta_0(\gamma+1)+(\gamma-1)^2}{2\sqrt{\gamma^2-2(1-\eta_0)\gamma+(\eta_0+1)^2}} - \frac{\gamma-1}{2}$.

Proof. The proof is largely inspired by Yang et al. [2020]. First, the solution to the ridge regression of student model is

$$W_2'^{\text{opt}} = \left(W_1'\mathbf{X}'\mathbf{X}'^T W_1'^T + \eta\mathbf{I}\right)^{-1} W_1'\mathbf{X}'\mathbf{X}'^T W.$$

Then the trained student model becomes

$$f_{W'}(x) = x^T W_1'^T W_2'^{\text{opt}} = x^T \Theta W,$$

where $\Theta = W_1'^T \left(W_1'\mathbf{X}'\mathbf{X}'^T W_1'^T + \eta\mathbf{I}\right)^{-1} W_1'\mathbf{X}'\mathbf{X}'^T \in \mathbb{R}^{d_w \times d_w}$.

Notice that $\Theta \perp W$ (since $W_1', \mathbf{X}' \perp W$), and X is an independent testing data, then

$$\begin{aligned} &\mathbb{E}_{X, W', W} \|f_{W'}(X) - f_W(X)\|^2 \\ &= \mathbb{E}_{X, \Theta, W} \|f_{W'}(X) - \mathbb{E}_{W'|W} [f_{W'}(X)]\|^2 + \mathbb{E}_{X, \Theta, W} \|\mathbb{E}_{W'|W} [f_{W'}(X)] - f_W(X)\|^2 \end{aligned} \quad (28)$$

$$\begin{aligned} &= \mathbb{E}_{X, \Theta, W} \|X^T \Theta W - \mathbb{E}_\Theta [X^T \Theta W]\|^2 + \mathbb{E}_{X, W} \|\mathbb{E}_\Theta [X^T \Theta W] - X^T W\|^2 \\ &= \mathbb{E}_{X, W, \Theta} \|X^T (\Theta - \mathbb{E}_\Theta [\Theta]) W\|^2 + \mathbb{E}_{X, W} \|X^T (\mathbb{E}_\Theta [\Theta] - \mathbf{I}) W\|^2 \\ &= \frac{1}{d_w} \mathbb{E}_{W, \Theta} \|(\Theta - \mathbb{E}_\Theta [\Theta]) W\|^2 + \frac{1}{d_w} \mathbb{E}_W \|(\mathbb{E}_\Theta [\Theta] - \mathbf{I}) W\|^2 \end{aligned} \quad (29)$$

$$\leq \frac{B}{d_w} \mathbb{E}_\Theta \|\Theta - \mathbb{E}_\Theta [\Theta]\|^2 + \frac{B}{d_w} \|\mathbb{E}_\Theta [\Theta] - \mathbf{I}\|^2 \quad (30)$$

$$= \frac{B}{d_w} \mathbb{E}_\Theta \|\Theta - \mathbf{I}\|^2, \quad (31)$$

where Eq. (28) is by the conditional bias-variance decomposition of $\mathbb{E}_{X, W', W} \|f_{W'}(X) - f_W(X)\|^2$, Eq. (29) is due to the fact that $\mathbb{E}[XX^T] = \frac{1}{d_w}\mathbf{I}$ and Eq. (30) is by $\mathbb{E}[\|W\|^2] \leq B$.

We now define

$$\tilde{\Theta} \triangleq W_1'^T \left(W_1' W_1'^T + \eta_0 \mathbf{I}\right)^{-1} W_1'.$$

Note that since $\mathbb{E}[\mathbf{X}'\mathbf{X}'^T] = \frac{1}{d_w}\mathbf{I}$, it is expected that when n, d_w are large enough, Θ will concentrate on $\tilde{\Theta}$. We now rigorously characterize their gap. Recall that $\eta = \frac{n}{d_w}\eta_0$,

$$\begin{aligned} \Theta - \tilde{\Theta} &= \frac{d_w}{n} W_1'^T \left(\frac{d_w}{n} W_1' \mathbf{X}' \mathbf{X}'^T W_1'^T + \eta_0 \mathbf{I} \right)^{-1} W_1' \mathbf{X}' \mathbf{X}'^T - W_1'^T \left(W_1' W_1'^T + \eta_0 \mathbf{I} \right)^{-1} W_1' \\ &= W_1'^T \left(W_1' \left(\frac{d_w}{n} \mathbf{X}' \mathbf{X}'^T - \mathbf{I} \right) W_1'^T + W_1' W_1'^T + \eta_0 \mathbf{I} \right)^{-1} W_1' \left(\frac{d_w}{n} \mathbf{X}' \mathbf{X}'^T - \mathbf{I} + \mathbf{I} \right) \\ &\quad - W_1'^T \left(W_1' W_1'^T + \eta_0 \mathbf{I} \right)^{-1} W_1' \\ &= W_1'^T \Delta_2 W_1' + W_1'^T (\Delta_2 + A) W_1' \Delta_1, \end{aligned}$$

where

$$\begin{aligned} \Delta_1 &= \frac{d_w}{n} \mathbf{X}' \mathbf{X}'^T - \mathbf{I}, \\ A &= \left(W_1' W_1'^T + \eta_0 \mathbf{I} \right)^{-1}, \\ \Delta_2 &= \left(W_1' \Delta_1 W_1'^T + W_1' W_1'^T + \eta_0 \mathbf{I} \right)^{-1} - A. \end{aligned}$$

Let $\|M\|_2$ be the spectral norm of a matrix M , then

$$\|\Theta - \tilde{\Theta}\|_2 \leq \|\Delta_2\|_2 \|W_1'\|_2^2 + \|\Delta_1\|_2 \|\Delta_2\|_2 \|W_1'\|_2^2 + \|\Delta_1\|_2 \|\tilde{\Theta}\|_2. \quad (32)$$

In addition, by a classical result on the perturbation of matrix inverse [Demmel, 1992], we have

$$\|\Delta_2\|_2 \leq \|A\|_2^2 \|\Delta_1\|_2 \|W_1'\|_2^2 + O\left(\|\Delta_1\|_2 \|W_1'\|_2^2\right).$$

Moreover, notice that $\|W_1'\|_2 = 1 + \sqrt{\frac{1}{\gamma}}$, $\|A\|_2 \leq \frac{1}{\eta_0}$ and $\|\tilde{\Theta}\|_2 = \frac{\sigma_{\max}(W_1')^2}{\sigma_{\max}(W_1')^2 + \eta_0} \leq 1$, where σ_{\max} is the largest singular value. Therefore, to have $\|\Theta - \tilde{\Theta}\|_2 = 0$, it is sufficient to show that $\|\Delta_1\|_2 \rightarrow 0$.

According to [Wainwright, 2019, Example 6.2], we have, with probability at least $1 - \delta$,

$$\|\Delta_1\|_2 \leq \left(\sqrt{\frac{d_w}{n}} + \sqrt{\frac{2}{n} \log \frac{1}{\delta}} + 1 \right)^2 - 1.$$

By setting $\delta = e^{-\frac{d_w}{2}}$, we have $\|\Delta_1\|_2 \rightarrow 0$ almost surely when $d_w, n \rightarrow \infty$.

Consequently, when $d_w, n \rightarrow \infty$, we have $\|\Theta - \tilde{\Theta}\|_2 = 0$ almost surely.

Furthermore, by Sherman-Morrison formula, we have

$$\|\tilde{\Theta} - \mathbf{I}\|^2 = \left\| \mathbf{I} - \left[\mathbf{I} - \left(\mathbf{I} + \eta_0^{-1} W_1'^T W_1' \right)^{-1} \right] \right\|^2 = \sum_{i=1}^{d_w} \frac{1}{\left(1 + \frac{\gamma}{\eta_0} \lambda_i \right)^2},$$

where $\lambda_i \geq 0$ is the i th eigenvalue of the matrix $M = \frac{d_w}{d_s} W_1'^T W_1'$.

Specifically, the eigenvalues $\{\lambda_i\}_{i=1}^{d_w}$ follow the Marchenko-Pasteur (MP) distribution when $d_w \rightarrow \infty$ [Marčenko and Pastur, 1967], which is defined as

$$P^{MP}(\lambda|\gamma) = \frac{1}{2\pi} \frac{\gamma \sqrt{(\gamma_+ - \lambda)(\lambda - \gamma_-)}}{\lambda} \mathbf{1}_{\lambda \in [\gamma_-, \gamma_+]},$$

where $\gamma_+ = (1 + \sqrt{1/\gamma})^2$ and $\gamma_- = (1 - \sqrt{1/\gamma})^2$.

Therefore, when $d_w \rightarrow \infty$ and $\gamma > 1$, we have

$$\begin{aligned} \frac{1}{d_w} \mathbb{E} \|\tilde{\Theta} - \mathbf{I}\|^2 &= \frac{1}{2\pi} \int_{\gamma_-}^{\gamma_+} \frac{\gamma \sqrt{(\gamma_+ - \lambda)(\lambda - \gamma_-)}}{\lambda \left(1 + \frac{\gamma}{\eta_0} \lambda \right)^2} d\lambda \\ &= \frac{\eta_0(\gamma + 1) + (\gamma - 1)^2}{2\sqrt{(\eta_0 + 1)^2 + 2(\eta_0 - 1)\gamma + \gamma^2}} - \frac{\gamma - 1}{2}. \end{aligned}$$

Putting everything together, we have

$$\begin{aligned}
\mathbb{E}_{X, W', W} \|f_{W'}(X) - f_W(X)\|^2 &= \frac{B}{d_w} \mathbb{E}_{W'_1, S'} \|\Theta - \mathbf{I}\|^2 \\
&= \frac{B}{d_w} \mathbb{E}_{W'_1} \|\tilde{\Theta} - \mathbf{I}\|^2 \\
&= \frac{\eta_0(\gamma + 1) + (\gamma - 1)^2}{2\sqrt{(\eta_0 + 1)^2 + 2(\eta_0 - 1)\gamma + \gamma^2}} - \frac{\gamma - 1}{2}.
\end{aligned}$$

This completes the proof. \square

C.3 Monotonicity Analysis

We prove that the function

$$h(\gamma, \eta_0) = \frac{\eta_0(\gamma + 1) + (\gamma - 1)^2}{2\sqrt{\gamma^2 - 2(1 - \eta_0)\gamma + (\eta_0 + 1)^2}} - \frac{\gamma - 1}{2},$$

in Theorem 4.1 is monotonically decreasing with $\gamma > 1$ when $\eta_0 > 0$.

Proof. Let $d(\gamma) = \sqrt{\gamma^2 - 2(1 - \eta_0)\gamma + (\eta_0 + 1)^2}$. We have

$$\begin{aligned}
h'(\gamma) &= \frac{2(2\gamma - 2 + \eta_0)d(\gamma) - [\eta_0(\gamma + 1) + (\gamma - 1)^2](2\gamma - 2 + 2\eta_0)d^{-1}(\gamma)}{4d^2(\gamma)} - \frac{1}{2} \\
&= \frac{(2\gamma - 2 + \eta_0)d^2(\gamma) - [\eta_0(\gamma + 1) + (\gamma - 1)^2](\gamma - 1 + \eta_0) - d^3(\gamma)}{2d^3(\gamma)} \\
&= \frac{k(\gamma)}{4d^3(\gamma)},
\end{aligned}$$

where $k(\gamma)$ is the numerator in the second line. Note that

$$\begin{aligned}
\lim_{\gamma \rightarrow 0} h(\gamma) &= 1, & \lim_{\gamma \rightarrow +\infty} h(\gamma) &= 0, \\
\lim_{\gamma \rightarrow 0} k(\gamma) &= -2\eta_0(\eta_0 + 1) < 0, & \lim_{\gamma \rightarrow +\infty} k(\gamma) &= 0.
\end{aligned}$$

The first three equations are obvious, and the fourth inequality requires exhaustive Taylor expansion and the L'Hospital's rule. To prove that $h(\gamma)$ is monotonically decreasing, we need to prove that $h'(\gamma) \leq 0$, which is equivalent to $k(\gamma) \leq 0$. Firstly, let $t = \gamma - 1 + \eta_0 > 0$ and there always holds

$$k'(\gamma) = 3t \left(t - \sqrt{t^2 + 4\eta_0} \right) + 6\eta_0 \geq 0.$$

Therefore, $k(\gamma)$ monotonically increases and approaches its maximum $\lim_{\gamma \rightarrow +\infty} k(\gamma) = 0$. In other words, $k(\gamma) < 0$, and $h'(\gamma) < 0$ for all $\gamma > 1$, which completes the proof. \square

D Omitted Proofs in Section 5

D.1 Proof of Corollary 5.1

We first restate Corollary 5.1 as follows.

Corollary 5.1. *Let $\phi(x) = \sum x_i \log x_i$ and define the reverse cross-entropy (RCE) as $\text{RCE}(y, \hat{y}) \triangleq -\sum_{i=1}^K \hat{y}_i \log y_i$ for any $y, \hat{y} \in \mathcal{Y}$, the following inequalities hold,*

$$\begin{aligned}
\mathbb{E}[\text{CE}(g(X), f_{W'}(X))] &\leq \mathbb{E}[\text{CE}(g(X), f_W(X))] - \mathbb{E}[\text{RCE}(f_W(X), f_{W'}(X))] + \mathbb{E}[H(f_{W'}(X))] + \epsilon_1, \\
\mathbb{E}[\text{RCE}(g(X), f_{W'}(X))] &\leq \mathbb{E}[\text{RCE}(g(X), f_W(X))] - \mathbb{E}[\text{CE}(f_W(X), f_{W'}(X))] + \mathbb{E}[H(f_{W'}(X))] + \epsilon_2,
\end{aligned}$$

where ϵ_1, ϵ_2 are defined as in Theorem 3.1.

Proof. Let $\phi(x) = \sum x_i \log x_i$, then D_ϕ becomes D_{KL} . Plugging $D_{\text{KL}}(y||\hat{y}) = \text{CE}(y, \hat{y}) - H(y)$ into Eq. (4), we have

$$\begin{aligned} & \mathbb{E}_{X,W'} [\text{CE}(g(X), f_{W'}(X))] - \mathbb{E}_X [H(g(X))] \\ & \leq \mathbb{E}_{X,W} [\text{CE}(g(X), f_W(X))] - \mathbb{E}_X [H(g(X))] \\ & \quad - \mathbb{E}_{X,W',W} [\text{RCE}(f_W(X), f_{W'}(X))] + \mathbb{E}_{X,W'} [H(f_{W'}(X))] + \epsilon_1. \end{aligned}$$

Hence,

$$\begin{aligned} \mathbb{E}_{X,W'} [\text{CE}(g(X), f_{W'}(X))] & \leq \mathbb{E}_{X,W} [\text{CE}(g(X), f_W(X))] \\ & \quad - \mathbb{E}_{X,W',W} [\text{RCE}(f_W(X), f_{W'}(X))] + \mathbb{E}_{X,W'} [H(f_{W'}(X))] + \epsilon_1. \end{aligned}$$

Similarly, substituting $D_{\text{KL}}(y||\hat{y}) = \text{CE}(y, \hat{y}) - H(y)$ into Eq. (5), we have

$$\begin{aligned} & \mathbb{E}_{X,W'} [\text{RCE}(g(X), f_{W'}(X))] - \mathbb{E}_{X,W'} [H(f_{W'}(X))] \\ & \leq \mathbb{E}_{X,W} [\text{RCE}(g(X), f_W(X))] - \mathbb{E}_{X,W} [H(f_W(X))] \\ & \quad - \mathbb{E}_{X,W',W} [\text{CE}(f_W(X), f_{W'}(X))] + \mathbb{E}_{X,W} [H(f_W(X))] + \epsilon_2. \end{aligned}$$

Hence,

$$\begin{aligned} \mathbb{E}_{X,W'} [\text{RCE}(g(X), f_{W'}(X))] & \leq \mathbb{E}_{X,W} [\text{RCE}(g(X), f_W(X))] \\ & \quad - \mathbb{E}_{X,W',W} [\text{CE}(f_W(X), f_{W'}(X))] + \mathbb{E}_{X,W'} [H(f_{W'}(X))] + \epsilon_2. \end{aligned}$$

This completes the proof. \square

D.2 Proof of Proposition 1

Proposition 1 (Restatement). *Under the ideal conditions of Corollary 3.1 where ϵ_1 and ϵ_2 vanish, the performance gain in the first inequality of Corollary 5.1 coincides with Eq. (6), while the gain in the second inequality is strictly smaller than Eq. (7).*

Proof. If $f_{W'}(x) = \mathcal{E}[f_W(x)|W']$ for $\forall x \in \mathcal{X}$, by Corollary 3.1 and Corollary 5.1, we have

$$\begin{aligned} \mathbb{E}_{X,W'} [\text{CE}(g(X), f_{W'}(X))] & = \mathbb{E}_{X,W} [\text{CE}(g(X), f_W(X))] - \mathbb{E}_{X,W',W} [\text{RCE}(f_W(X), \mathcal{E}[f_W(X)|W', X])] \\ & \quad + \mathbb{E}_{X,W'} [H(\mathcal{E}[f_W(X)|W', X])] \\ & = \mathbb{E}_{X,W} [\text{CE}(g(X), f_W(X))] - \mathbb{E}_{X,W,W'} [\text{D}_{\text{KL}}(\mathcal{E}[f_W(X)|W', X]||f_W(X))]. \end{aligned}$$

Thus, here the misfit term $\mathbb{E}_{X,W,W'} [\text{D}_{\text{KL}}(\mathcal{E}[f_W(X)|W', X]||f_W(X))]$ matches the misfit term in Eq. (6).

In addition, if $f_{W'}(x) = \mathbb{E}[f_W(x)|W']$ for $\forall x \in \mathcal{X}$, by Corollary 3.1 and Corollary 5.1, we have

$$\begin{aligned} \mathbb{E}_{X,W'} [\text{RCE}(g(X), f_{W'}(X))] & = \mathbb{E}_{X,W} [\text{RCE}(g(X), f_W(X))] - \mathbb{E}_{X,W',W} [\text{CE}(f_W(X), \mathbb{E}[f_W(X)|W', X])] \\ & \quad + \mathbb{E}_{X,W'} [H(\mathbb{E}[f_W(X)|W', X])] \\ & = \mathbb{E}_{X,W} [\text{RCE}(g(X), f_W(X))] - \mathbb{E}_{X,W',W} [\text{D}_{\text{KL}}(f_W(X)||\mathbb{E}[f_W(X)|W', X])] \\ & \quad - \mathbb{E}_{X,W} [H(f_W(X))] + \mathbb{E}_{X,W'} [H(\mathbb{E}[f_W(X)|W', X])]. \end{aligned}$$

Since entropy is a concave function, we have $\mathbb{E}_{X,W'} [H(\mathbb{E}[f_W(X)|W', X])] \geq \mathbb{E}_{X,W} [H(f_W(X))]$. As a result, the performance gain between $\mathbb{E}_{X,W'} [\text{RCE}(g(X), f_{W'}(X))]$ and $\mathbb{E}_{X,W} [\text{RCE}(g(X), f_W(X))]$ is larger than that in Eq. (7).

This completes the proof. \square

D.3 Proof of Proposition 2

Proposition 2 (Restatement). *Given a data distribution $\mu = \mu_X \mu_{Y|X}$ and any $\alpha \in [0, 1]$, we define a label-shifted distribution $\hat{\mu} = \mu_X \hat{\mu}_{\hat{Y}|X}$ by smoothing the labels as follows: for each $(X, Y) \sim \mu$, the smoothed label is given by $\hat{Y}_j = \frac{1}{2} + \alpha(Y_j - \frac{1}{2})$ for $\forall j \in [2]$. If RCE is used as the loss function in binary classification, then the population risk minimizer on $\hat{\mu}$ also minimizes the population risk on μ .*

Proof. Given any model $f : \mathcal{X} \rightarrow \mathcal{Y}$, define the population risk using reverse cross-entropy as

$$R_{rce}(f) = -\mathbb{E}_X \sum_i [f(X)]_i \log Y_i,$$

$$R_{rce}^\alpha(f) = -\mathbb{E}_X \sum_i [f(X)]_i \log Y'_i = -\mathbb{E}_X \sum_i [f(X)]_i \log \left(\frac{1}{K} + \alpha \left(Y_i - \frac{1}{K} \right) \right),$$

where supervision $Y = [Y_1, \dots, Y_K]^T$ that satisfies $\|Y\|_1 = 1$. Therefore,

$$\begin{aligned} R_{rce}^\alpha(f) - R_{rce}(f) &= \mathbb{E}_X \sum_i [f(X)]_i \log \underbrace{\frac{Y_i}{\frac{1}{K} + \alpha \left(Y_i - \frac{1}{K} \right)}}_{q_\alpha(Y_i)} \\ &= \mathbb{E}_X \sum_i [f(X)]_i q_\alpha(Y_i). \end{aligned} \quad (33)$$

Note that $q_\alpha(Y_i) = \log \frac{Y_i}{\frac{1}{K} + \alpha \left(Y_i - \frac{1}{K} \right)} = \log \frac{1}{\alpha} \left(1 - \frac{1-\alpha}{1-\alpha+\alpha K Y_i} \right)$ is a monotonically increasing function of Y_i . Let the minimizer of the ambiguous weak supervision

$$f_\star = \arg \min_f R_{rce}^\alpha(f).$$

There always hold $R_{rce}^\alpha(f) \geq R_{rce}^\alpha(f_\star)$. Without loss of generality, let $Y_h = 1 - \epsilon$, where $\epsilon \rightarrow 0$. For the binary classification case, i.e., $K = 2$, the inequality $R_{rce}^\alpha(f) \geq R_{rce}^\alpha(f_\star)$ means

$$\begin{aligned} -\mathbb{E}_X \sum_i [f(X)]_i \log Y'_i &\geq -\mathbb{E}_X \sum_i [f_\star(X)]_i \log Y'_i \\ \Rightarrow \mathbb{E}_X \sum_i [f_\star(X) - f(X)]_i \log Y'_i &\geq 0 \\ \Rightarrow \mathbb{E}_X [f_\star(X) - f(X)]_h \log Y'_h + \mathbb{E}_X [f_\star(X) - f(X)]_{1-h} \log Y'_{1-h} &\geq 0 \\ \Rightarrow \mathbb{E}_X [f_\star(X) - f(X)]_h \log Y'_h - \mathbb{E}_X [f_\star(X) - f(X)]_h \log(1 - Y'_h) &\geq 0 \\ \Rightarrow \mathbb{E}_X [f_\star(X) - f(X)]_h \log \frac{Y'_h}{1 - Y'_h} &\geq 0 \\ \Rightarrow \mathbb{E}_X [f_\star(X) - f(X)]_h &\geq 0 \\ \Rightarrow \mathbb{E}_X [f_\star(X) - f(X)]_{1-h} &\leq 0 \end{aligned}$$

By substituting f_\star into Eq. (33) and we derive an additional similar equation. Combining this new equation with the original Eq. (33) yields the below results:

$$\begin{aligned} &[R_{rce}^\alpha(f) - R_{rce}(f)] - [R_{rce}^\alpha(f_\star) - R_{rce}(f_\star)] \\ &= [R_{rce}^\alpha(f) - R_{rce}^\alpha(f_\star)] - [R_{rce}(f) - R_{rce}(f_\star)] \\ &= \mathbb{E}_X \sum_i [f(X) - f_\star(X)]_i q_\alpha(Y_i) \\ &= \mathbb{E}_X [f(X) - f_\star(X)]_h q_\alpha(Y_h) + \mathbb{E}_X [f(X) - f_\star(X)]_{1-h} q_\alpha(Y_{1-h}) \\ &= \mathbb{E}_X [f_\star(X) - f(X)]_{1-h} q_\alpha(Y_h) + \mathbb{E}_X [f(X) - f_\star(X)]_{1-h} q_\alpha(Y_{1-h}) \quad (\|f_\star(X)\|_1 = 1) \\ &= \mathbb{E}_X [f(X) - f_\star(X)]_{1-h} [q_\alpha(Y_{1-h}) - q_\alpha(Y_h)]. \end{aligned}$$

We have $Y_{1-h} \leq Y_h$, which means $q_\alpha(Y_{1-h}) \leq q_\alpha(Y_h)$. Also, $\mathbb{E}_X [f(X)]_{1-h} \geq \mathbb{E}_X [f_\star(X)]_h$. It leads to $[R_{rce}^\alpha(f) - R_{rce}^\alpha(f_\star)] - [R_{rce}(f) - R_{rce}(f_\star)] \leq 0$, i.e.,

$$0 \leq R_{rce}^\alpha(f) - R_{rce}^\alpha(f_\star) \leq R_{rce}(f) - R_{rce}(f_\star).$$

Thus, $R_{rce}(f_\star) \leq R_{rce}(f)$ holds for any f , which contributes to the final result

$$f_\star = \arg \min_f R_{rce}(f).$$

□

D.4 Gradient Analysis

In the setting of predictive uncertainty, to further demonstrate the advantage of RCE described in Section 5, we introduce a gradient analysis for forward CE/KL and reverse CE/KL losses, which are shown in Eq. (34)-(37).

$$\frac{\partial \text{CE}(g(X), f_{W'}(X))}{\partial [f_{W'}(X)]_j} = -\frac{\partial \sum_{i=1}^2 [g(X)]_i \log [f_{W'}(X)]_i}{\partial [f_{W'}(X)]_j} = -\frac{[g(X)]_j}{[f_{W'}(X)]_j} + \frac{1 - [g(X)]_j}{1 - [f_{W'}(X)]_j}, \quad (34)$$

$$\frac{\partial \text{D}_{\text{KL}}(g(X) || f_{W'}(X))}{\partial [f_{W'}(X)]_j} = \frac{\partial \text{CE}(g(X), f_{W'}(X)) - \partial H(g(X))}{\partial [f_{W'}(X)]_j} = \frac{\partial \text{CE}(g(X), f_{W'}(X))}{\partial [f_{W'}(X)]_j}, \quad (35)$$

$$\frac{\partial \text{RCE}(g(X), f_{W'}(X))}{\partial [f_{W'}(X)]_j} = -\frac{\partial \sum_{i=1}^2 [f_{W'}(X)]_i \log [g(X)]_i}{\partial [f_{W'}(X)]_j} = \log \frac{1 - [g(X)]_j}{[g(X)]_j}. \quad (36)$$

$$\frac{\partial \text{D}_{\text{KL}}(f_{W'}(X) || g(X))}{\partial [f_{W'}(X)]_j} = \log \frac{1 - [g(X)]_j}{[g(X)]_j} - \log \frac{1 - [f_{W'}(X)]_j}{[f_{W'}(X)]_j} \quad (37)$$

As the student prediction $f_{W'}(x)$ approaches the supervision $g(x)$, the gradients for forward CE/KL and reverse KL diminish to zero. In contrast, the reverse CE gradient persists, maintaining non-vanishing values that facilitate more robust learning under uncertain supervision. It will be empirically validated in Appendix E.3.

E Experimental Details and Additional Results

E.1 Experimental Details

Dataset Processing For standard NLP tasks (SciQ [Welbl et al., 2017], Amazon Polarity [McAuley and Leskovec, 2013] and Twitter Sentiment), we convert the original questions and candidate answers Q, A_1, \dots, A_k into multiple question-answer pairs (Q, A_i) , where correct answers are labeled as positive and incorrect ones as negative. For reward modeling tasks (CAI-Harmless [Bai et al., 2022b], HH-RLHF [Bai et al., 2022a]), we directly pair the chosen and rejected responses while maintaining their original preference labels. All datasets maintain class balance and are partitioned into three subsets: S, S' , and S_{test} , designed for weak model training, strong model training, and final performance evaluation, respectively.

Model Architecture For standard NLP tasks (SciQ, Amazon Polarity, Twitter Sentiment), with experimental setup of Burns et al. [2023], we add a two-dimensional linear projection layer atop the pretrained model’s final representations, followed by a Softmax function to obtain the final prediction probabilities. For reward modeling tasks (CAI-Harmless, HH-RLHF), with experimental settings referencing Yao et al. [2025a,b], we instead use a single-output linear layer with a Sigmoid activation to map the output to a probability in $[0, 1]$, indicating whether the response meets the harmlessness or helpfulness criteria.

Training Configurations We implement early stopping to prevent overfitting, using minimal training epochs for efficiency [Burns et al., 2023]. Standard NLP tasks train for 2 epochs while reward modeling tasks use only 1 epoch. The base learning rate is set to 1×10^{-5} , except for GPT2 and GPT2-Medium models on SciQ and Amazon Polarity datasets which employ 5×10^{-5} . Batch sizes are configured as 32 for NLP tasks and 16 for reward modeling tasks. All experiments run on 4 NVIDIA vGPUs (32GB) with at least three independent random seeds for reproducibility. Complete configurations are summarized in Table 2. Notably, we adopt a full fine-tuning strategy during training without freezing any pretrained parameters, allowing the model to fully adapt to downstream tasks.

Table 2: Training Configurations on Different Datasets.

Dataset	$ S $	$ S' $	$ S_{\text{test}} $	Max Seq Len	Epochs	Batch Size
SciQ	5839	5838	1000	1024	2	32
Amazon Polarity	5000	5000	1000	1024	2	32
Twitter Sentiment	7000	7000	1000	1024	2	32
CAI-Harmless	4000	4000	4000	512	1	16
HH-RLHF	4000	4000	4000	512	1	16

Loss Fuctions The Confidence-Adaptive Cross Entropy (CACE) loss dynamically combines reverse cross-entropy (RCE) and standard cross-entropy (CE) based on teacher confidence levels. Formally, it is defined as:

$$\mathcal{L}_{\text{CACE}}(y, \hat{y}) = \mathbb{I}(y, c) \cdot \text{RCE}(y, \hat{y}) + (1 - \mathbb{I}(y, c)) \cdot \text{CE}(y, \hat{y}), \quad (38)$$

where \hat{y} represents the student’s prediction and $\mathbb{I}(y, c)$ is an indicator function that activates when the teacher’s soft label y has confidence below threshold c . For our binary classification tasks, we quantify confidence as $|y - 0.5|$, where $y \in (0, 1)$ is the teacher’s soft label. The threshold c is determined adaptively before W2S training by selecting a quantile such that exactly $\eta\%$, of the samples are viewed as low-confidence, i.e., activate $\mathbb{I}(y, c)$. In our experiments, $\eta \in \{5, 10, 20, 30\}$.

The Symmetric Cross Entropy Loss (SL) [Wang et al., 2019] is designed to handle noisy labels by balancing reverse cross-entropy (RCE) and standard cross-entropy (CE). It is formally defined as:

$$\mathcal{L}_{\text{SL}}(y, \hat{y}) = \lambda_1 \cdot \text{RCE}(y, \hat{y}) + \lambda_2 \cdot \text{CE}(y, \hat{y}), \quad (39)$$

where \hat{y} represents the student’s prediction, and λ_1 and λ_2 are weighting factors that adjust the contributions of RCE and CE respectively. In our experiments, we evaluate the performance of SL under different configurations of $(\lambda_1, \lambda_2) \in \{(1.0, 0.5), (1.0, 0.1), (1.0, 1.0), (0.5, 1.0), (0.1, 1.0)\}$.

The Auxiliary Confidence Loss (AUX) [Burns et al., 2023] is primarily aimed at enhancing the confidence of the student model’s predictions through regularization. It is defined as:

$$\mathcal{L}_{\text{AUX}} = \beta \text{CE}(f_w(x), f_{w'}(x)) + (1 - \beta) \text{CE}(f_{w'}(x), \hat{f}_{w'}(x)), \quad (40)$$

where $\text{CE}(\cdot, \cdot)$ denotes the cross-entropy loss between two prediction distributions. Here, $f_w(x)$ represents the weak label prediction from one model, $f_{w'}(x)$ is the prediction from another weakly supervised model, and $\hat{f}_{w'}(x)$ is the hardened prediction of the student model, which becomes a one-hot vector when $f_{w'}(x)$ exceeds a certain confidence threshold. Following Burns et al. [2023], the confidence threshold t is adjusted so that exactly half of the samples in a batch have $f(x) > t$, ensuring that only sufficiently confident predictions are considered for hardening. Additionally, the weight parameter β undergoes a linear warm-up phase, increasing from 0 to its maximum value β_{\max} during the initial training period. For our experiments, we apply this warm-up strategy separately over the first 20%, 50%, and 100% of the training data.

Notably, the results for CACE, SL, and AUX shown in Table 1 are the best outcomes selected from the above-mentioned hyperparameter settings.

E.2 Bias and Variance Estimation in W2SG

Following Yang et al. [2020], we provide the bias-variance decomposition for cross-entropy (CE) in our work, which is formally given by:

$$\underbrace{\mathbb{E}_X \mathbb{E}_\theta [\text{CE}(g(X), f_\theta(X))]}_{\text{Population Risk}} = \underbrace{\mathbb{E}_X [\text{D}_{\text{KL}}(g(X) \| \mathcal{E}_\theta[f_\theta(X)])]}_{\text{Bias}^2} + \underbrace{\mathbb{E}_X \mathbb{E}_\theta [\text{D}_{\text{KL}}(\mathcal{E}_\theta[f_\theta(X)] \| f_\theta(X))]}_{\text{Variance}}, \quad (41)$$

where the model parameter $\theta \in \{W, W'\}$, and the intrinsic randomness of θ stems from several sources, such as data sampling, model initialization and optimization. Here, X denotes a sample from the test set. $\mathcal{E}_\theta[f_\theta(X)]$ is the average of log-probability after normalization.

To accurately estimate $\mathcal{E}_\theta[f_\theta(X)]$ in Eq. (41), we train multiple independent teacher-student pairs on distinct subsets sampled from large-scale datasets and average their performance. Specifically, we construct five disjoint 10000-sample subsets from Amazon Polarity (with equal halves allocated to weak model training and W2S training), training five teacher-student pairs across four random seeds. Similarly, we extract three 14000-sample subsets from Twitter Sentiment, conducting experiments across five random seeds. The complete implementation details are provided in Algorithm 1, and the results are shown as solid lines in Figure 1.

To validate Corollary 3.1 – which states that W2SG emerges when the student’s prediction matches its (dual) posterior mean teacher – we implement a probability-based ensemble [Dietterich, 2000; Zhou, 2025] of multiple weak teachers for student supervision. Specifically, we compute the dual expectation $\mathcal{E}[f_W(X)]$ over weak teachers’ predictions to approximate the teacher’s conditional expectation $\mathcal{E}[f_W(X)|W', X]$ in Eq. (6). When using CE loss for teacher training, $\mathcal{E}[f_W(X)]$ is computed as:

$$\mathcal{E}[f_W(X)] = \frac{\exp(\mathbb{E}_W[\log f_W(X)])}{\sum_{i=1}^K \exp(\mathbb{E}_W \log [f_W(X)]_i)}, \quad (42)$$

where $[f_W(X)]_i$ denotes the probability of sample X belonging to class i as predicted by the teacher model, and K represents the total number of classes. Note that in this context, X represents a fixed sample from the W2S training set, and the expectation is taken only over the weak teachers. We use these ensemble predictions as training data to supervise student models, with the results presented as dashed lines in Figure 1.

Algorithm 1 Estimate W2SG Bias and Variance

Input: Test point \mathbf{x} , weak model training set S and strong model training set S'

for $i = 1$ **to** k **do**

Split the (S, S') into N pairs: $(S_1^{(i)}, S_1'^{(i)}), \dots, (S_N^{(i)}, S_N'^{(i)})$

for $j = 1$ **to** N **do**

Train the weak model f_w using $S_j^{(i)}$

Evaluate the weak model at \mathbf{x} ; call the result $\pi_j^{(i)}$

Generate pseudo-labels for $S_j'^{(i)}$ using f_w

Train the strong model using $S_j'^{(i)}$

Evaluate the W2S model at \mathbf{x} ; call the result $\pi_j'^{(i)}$;

end for

end for

Compute $\hat{\pi} = \exp \left\{ \frac{1}{N \cdot k} \sum_{ij} \log \left(\pi_j^{(i)} \right) \right\}$, $\hat{\pi}' = \exp \left\{ \frac{1}{N \cdot k} \sum_{ij} \log \left(\pi_j'^{(i)} \right) \right\}$

(using element-wise log and exp; $\hat{\pi}$ estimates $\bar{\pi}$).

Normalize $\hat{\pi}$ to get a probability distribution.

Compute the variance $\frac{1}{N \cdot k} \sum_{ij} \text{D}_{\text{KL}} \left(\hat{\pi} \| \pi_j^{(i)} \right)$, $\frac{1}{N \cdot k} \sum_{ij} \text{D}_{\text{KL}} \left(\hat{\pi}' \| \pi_j'^{(i)} \right)$.

Compute the bias $\frac{1}{N \cdot k} \sum_{ij} \text{D}_{\text{KL}} \left(\pi_0 \| \hat{\pi} \right)$, $\frac{1}{N \cdot k} \sum_{ij} \text{D}_{\text{KL}} \left(\pi_0 \| \hat{\pi}' \right)$.

where $\pi_0(\mathbf{x})$ be the one-hot encoding of the ground-truth label.

E.3 Additional Empirical Validation of RCE’s Robustness to Predictive Uncertainty

Gradient Dynamics in CE and RCE In addition to the Amazon Polarity and HH-RLHF datasets presented in Figure 2, we further compare the sensitivity of CE and RCE losses to predictive uncertainty on SciQ and CAI-Harmless datasets. We observe that models trained with RCE tend to move farther in the parameter space. As shown in Figure 2 and Figure 3, nearly all RCE Distance values (purple line) are higher than CE Distance values (green line). When $\alpha = 0$, $\mathcal{L}_{\text{RCE}} = \log K$ becomes constant for K -classification, resulting in zero gradient and thus RCE Distance equals zero. We further track the training dynamics via gradient norm and gradient direction variance (GDV) [Liu et al., 2023], where the GDV metric quantifies the directional consistency of mini-batch gradients during training.

$$\text{GDV} = \frac{1}{|G| \cdot (|G| - 1)} \sum_{g_i, g_j \in G, i \neq j} \left(1 - \frac{\langle g_i, g_j \rangle}{\|g_i\|_2 \cdot \|g_j\|_2} \right), \quad (43)$$

where G denotes a set of mini-batch gradients. As shown in Figure 4, although RCE has smaller gradient norms, its GDV remains low, suggesting more consistent update directions. Conversely, CE exhibits higher GDV, leading to more “meandering” updates and causing the model to “wander” around the initial point.

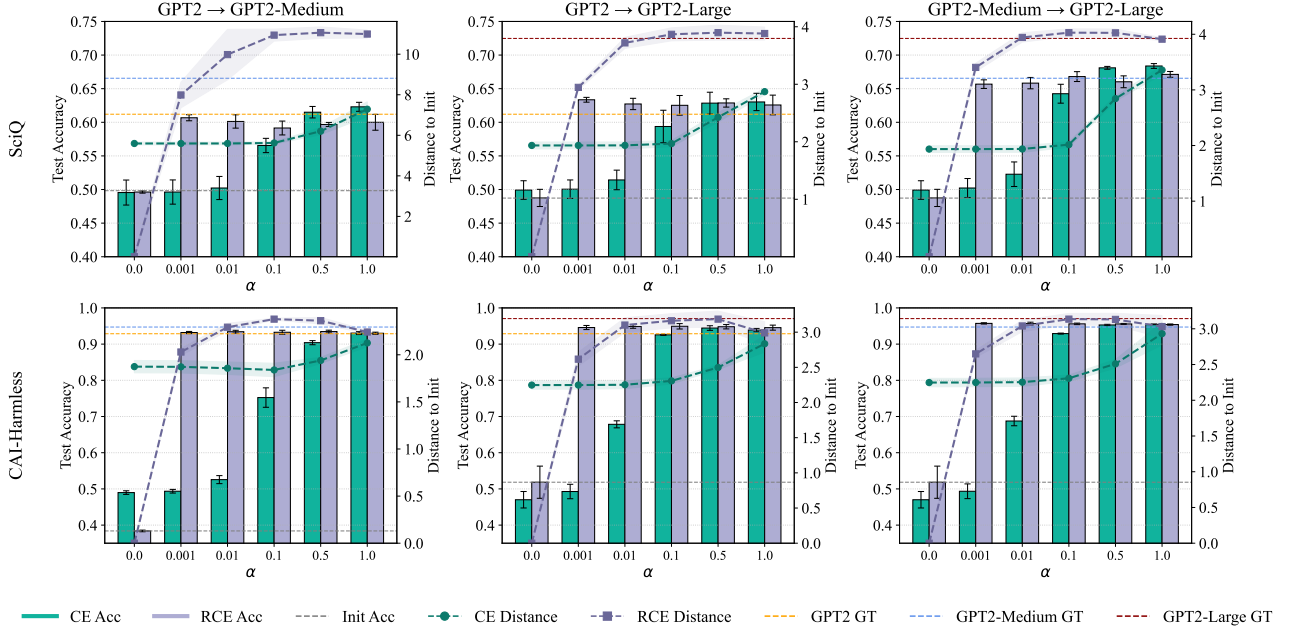


Figure 3: Performance of the GPT2 series models across SciQ and CAI-Harmless under varying α values, comparing CE and RCE losses. “GPT2 \rightarrow GPT2-Medium” denotes GPT2 supervising GPT2-Medium. Left y-axis shows test accuracy, corresponding to the bar plots for CE Acc and RCE Acc. Right y-axis illustrates the L_2 norm between the fine-tuned and initial models, represented by the line plots for CE Distance and RCE Distance. The cases $\alpha = 0$ and $\alpha = 1$ represent uniform and unshifted pseudo-labels, respectively. GT denotes the test accuracy achieved by training with ground truth labels. All experiments are repeated three times.

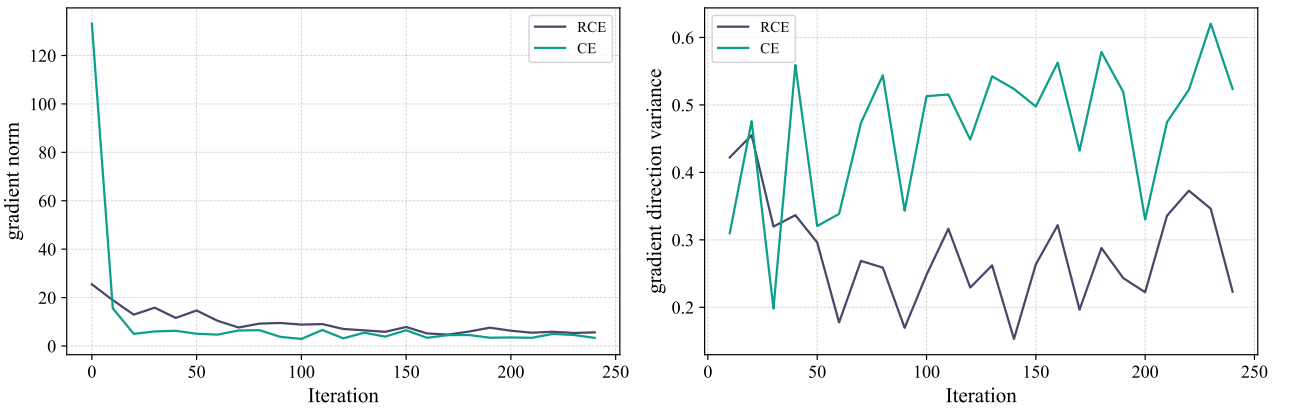


Figure 4: Gradient norm (left) and gradient direction variance (GDV, right) on the CAI-Harmless dataset, where GPT2-Medium is supervised by GPT2. RCE demonstrates lower GDV than CE, indicating stronger gradient consistency.

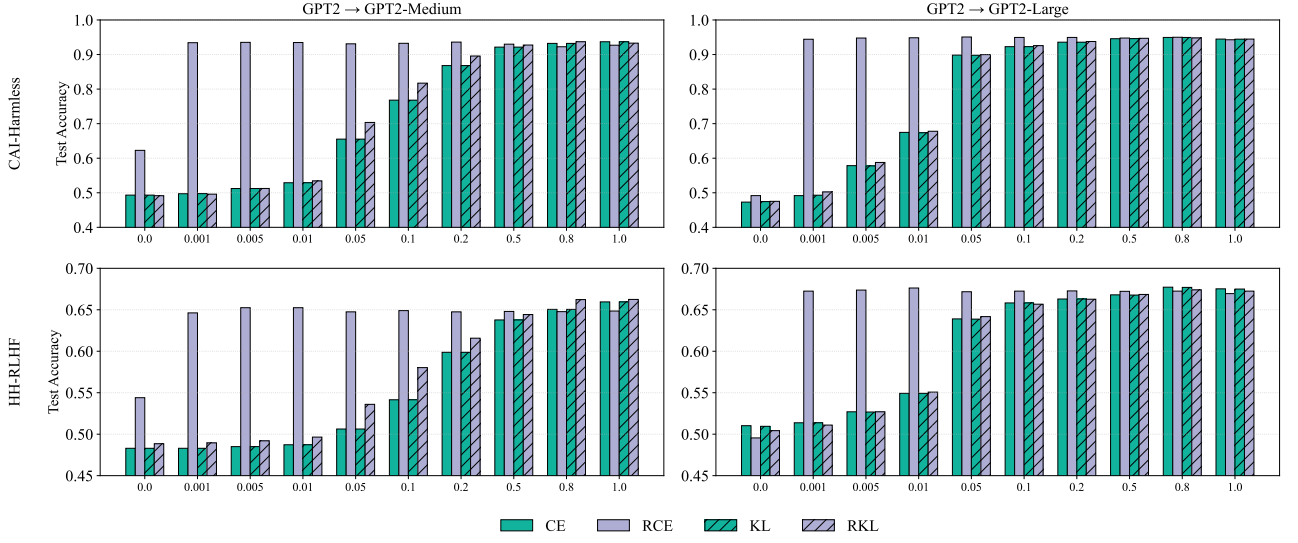


Figure 5: Performance of the GPT2 series models across CAI-Harmless and HH-RLHF under varying α values, comparing CE, RCE, KL and RKL losses. “GPT2-Medium \rightarrow GPT2” denotes GPT2-Medium supervising GPT2. The cases $\alpha = 0$ and $\alpha = 1$ represent uniform and unshifted pseudo-labels, respectively.

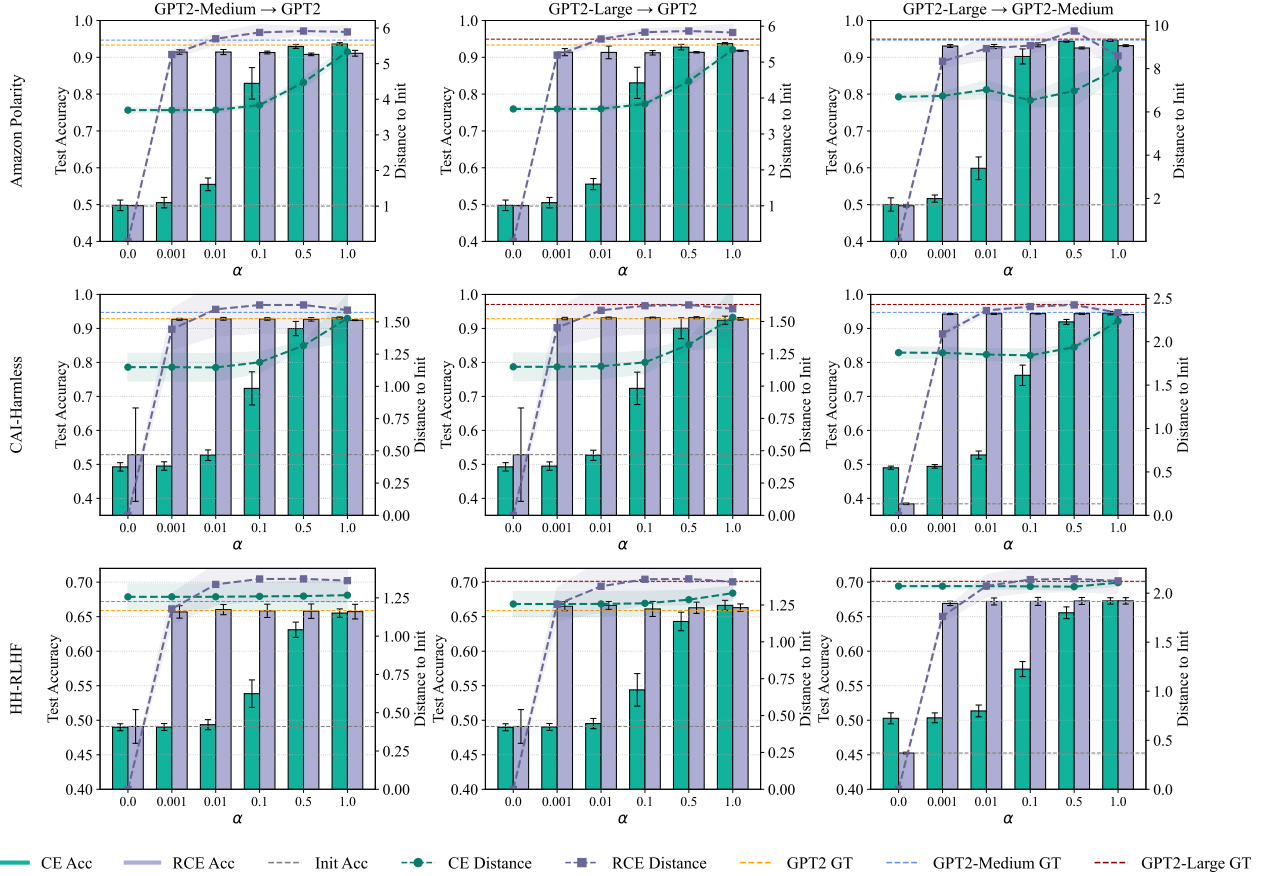


Figure 6: Performance of the GPT2 series models across Amazon Polarity, CAI-Harmless and HH-RLHF under varying α values, comparing CE and RCE losses. “GPT2-Medium \rightarrow GPT2” denotes GPT2-Medium supervising GPT2. Left y-axis shows test accuracy, corresponding to the bar plots for CE Acc and RCE Acc. Right y-axis illustrates the L_2 norm between the fine-tuned and initial models, represented by the line plots for CE Distance and RCE Distance. The cases $\alpha = 0$ and $\alpha = 1$ represent uniform and unshifted pseudo-labels, respectively. GT denotes the test accuracy achieved by training with ground truth labels. All experiments are repeated three times.

Comparison of CE, RCE, KL and RKL in W2SG Prior works [Yao et al., 2025a] investigated the mode-seeking behavior [Minka et al., 2005] of reverse KL divergence (RKL) in W2SG, establishing its advantages. We further conduct a systematic comparison of CE, RCE, KL, and RKL when applying the label-proportional smoothing strategy as outlined in Proposition 2. As shown in Fig. 5, RCE demonstrates significantly stronger robustness to predictive uncertainty compared to the other three losses on both CAI-Harmless and HH-RLHF datasets. This empirically validates Proposition 2 and Appendix D.4 regarding RCE’s gradient stability advantages, despite RKL differing from RCE by only an entropy term.

Comparison of CE and RCE in Knowledge Distillation We also investigate RCE under standard knowledge distillation [Hinton et al., 2015] settings, where a high-complexity teacher model supervises a low-complexity student model. Specifically, we consider two setups: (1) GPT2-Medium serves as the teacher, providing pseudo-labels to supervise GPT2; and (2) GPT2-Large supervises both GPT2 and GPT2-Medium. Results are summarized in Figure 6. Consistent with our findings in W2SG, RCE maintains significantly higher accuracy on samples with low-confidence predictions compared to CE. Models trained with RCE exhibit more consistent gradient directions and achieve larger parameter updates during training, indicating better learning stability and efficiency.